A WIND TUNNEL INVESTIGATION OF THE AERODYNAMIC CHARACTERISTICS OF HIGH-LIFT DEVICES ON SUPERSONIC WINGS AT LOW SUBSONIC SPEED

Thesis by

Philip G. Blenkush

In Partial Fulfillment of the Requirements

For the Degree of

Aeronautical Engineer

California Institute of Technology

Pasadena, California

1949

ACKNOWLEDGEMENTS

The author wishes to express gratitude to Mr. Henry T. Nagamatsu for his continued advice and helpful guidance in the preparation of this thesis.

The author is also indebted to co-worker, Mr. James E. Densmore, who assisted in the experimental work and supplied photographic equipment for the tuft flow studies.

ABSTRACT

An investigation was made to determine the effects of various full- and partial-span high-lift devices on the lift, drag, and pitching moment characteristics of a straight wing and a highly sweptforward wing, both having an aspect ratio of 1.72 and a thin double wedge symmetrical airfoil section. Split, extended leading edge, and extended trailing edge flaps were tested at various deflection angles on each wing alone and also on wing-fuselage combinations. In addition, plain leading edge flaps extending over a portion of the outboard span were tested on the sweptforward wing. Tuft surveys were made on typical model configurations to determine the change in stall pattern due to variation in the angle of attack.

From the results of the tests it was found that a given flap configuration produced approximately equal increments of maximum lift on the sweptforward wing alone and on the same wing combined with a fuselage. Comparison of the results obtained with the straight wing showed that the maximum lift increments were lower for a given flap used on wing plus fuselage than those obtained with the same flap on the basic straight wing. When considered from the maximum lift standpoint, the extended trailing edge flap was superior to either split or extended leading edge flap. Reduced span flaps were not as effective on the

sweptforward wing as the comparable full span flap. In the case of the straight wing alone, reduced span split and extended trailing edge flaps produced higher maximum lifts than did the corresponding full span configuration. This effect was also observed with the split flap tests on the straight wing combined with the fuselage.

The experimental work was performed in the Cal Tech-Merrill wind tunnel located on the Pasadena City College campus.

TABLE OF CONTENTS

I. INTRODUCTION

Progress into the realm of transonic and supersonic flight in the past few years has brought about radical changes in the configuration of aircraft designed for such speeds. Aerodynamic considerations dictate the use of highly swept wings having a thin airfoil section of zero camber with a sharp leading edge. The efficient structural design requires that the wing have a fairly low aspect ratio.

The above requirements introduce new aerodynamic problems at low subsonic flight speeds. It is well known that a thin wing having a sharp leading edge and little or no camber will have a relatively low maximum lift coefficient. Reduced aspect ratio decreases the lift curve slope and increases the angle of attack for maximum lift. Additional low speed aerodynamic problems are introduced when highly swept wings are used.

This investigation was undertaken with the primary objective of obtaining systematic results for various high-lift devices at low subsonic speed. Results for a delta wing and a sweptback wing, both having an aspect ratio of 1.72 and a sweep angle of 65 degrees at the leading edge, are reported in Ref. 1. This investigation is a continuation of that program with studies being made on a highly sweptforward wing and a straight wing both

having an aspect ratio of 1.72. Tests were made on wings alone and also in combination with a body similar to what might be found on an aircraft designed for flight in the transonic or supersonic regime.

All tests were made in the two- by four-foot closed-throat low speed Cal Tech-Merrill wind tunnel located on the Pasadena City College campus.

II. DESCRIPTION OF MODELS AND EQUIPMENT

The sweptforward wing model is shown in Fig. 1. It is the identical model that was tested as a sweptback wing in Ref. 1. The principal geometric features of this wing are as follows: (Dimensions listed in terms of chord are with reference to the chord parallel to the direction of the relative wind in symmetrical flight.)

Sweep angle of the leading edge	55° forward
Sweep angle of the line through the 50 per cent chord points	61° forward
Airfoil section	Double wedge symmetrical
Maximum thickness location	0.5 chord
Maximum thickness, at wing root at wing tip	0.05 chord 0.02 chord
Root chord length, c_r	10.0 inches
Tip chord length, c_t	5.13 inches
Mean aerodynamic chord, $\bar{c}$	7.84 inches
Taper ratio, c_t/c_r	0.513
Span, b	13.0 inches
Area, S	98.35 sq. in.
Aspect ratio, b^2/S	1.72

The wing was equipped with lateral control surfaces for the sweptback configuration (Cf. Fig. 1). In the sweptforward attitude these were tested as plain leading edge partial span flaps.

A drawing of the straight wing model is given in Fig. 2. This wing was constructed of mahogony to the following dimensions:

Sweep angle of the leading edge	13° sweepback
Sweep angle of the line through the 50 per cent chord points	0°
Airfoil section	Double wedge symmetrical
Maximum thickness location	0.5 chord
Maximum thickness, at wing root at wing tip	0.05 chord 0.02 chord
Root chord length, c_r	9.08 inches
Tip chord length, c_t	6.04 inches
Mean aerodynamic chord, $\bar{c}$	7.54 inches
Taper ratio, c_t/c_r	0.665
Span, b	13.0 inches
Area, S	98.3 sq. in.
Aspect ratio, b^2/S	1.72

The fuselage tested in combination with the wings is described in Ref. 2. This fuselage was also used in the tests reported in Ref. 1. A conical nose piece 6.23 inches long and having an apex angle of 30 degrees was fabricated to provide an alternative fuselage configuration representative of a rocket propelled vehicle. Figs. 3 and 4 show typical wing-fuselage combinations. Fig. 5 gives the principal dimensions of the horizontal tail surfaces which were tested on the wing-fuselage models.

The high-lift devices tested were as follows: plain leading edge partial span flaps located outboard (swept-forward wing only); extended leading edge flaps; extended trailing edge flaps; and split flaps. The plain leading edge partial span flaps were cut out from the extreme tip of the sweptforward wing and were intended to be used as ailerons for this wing in the sweptback configuration. These flaps were held in the deflected position by means of scotch tape and dural sheet stock bent to the appropriate angle. The remaining flap types mentioned above were cut and bent from 0.020 inch phosphor-bronze sheet stock. These were secured in place by scotch tape. Fig. 6 indicates the reference plane from which angular displacement for each type of flap was measured. Detailed information on the dimensions for all of the above flaps is given in the Code of Model Configurations on page 24 of this report.

The test program was carried out in the two- by four-foot closed-throat Cal Tech-Merrill wind tunnel located on the Pasadena City College campus. The tunnel operates at a maximum dynamic pressure of 13.5 pounds per square foot or approximately 80 miles per hour. Speed adjustments are made by means of a step-type rheostat control which regulates the supply voltage to the electric motor driving the wind tunnel fan.

The force measurements were made on a portable three-component balance system usually used with this tunnel. The models were mounted upright on a three-strut support system. Each force component was measured by means of a single beam balance. These balances were brought to equilibrium manually by first shifting calibrated weights on the notched main beam and then adjusting a small weight by means of a worm and screw for the final balance.

III. DESCRIPTION OF THE TEST PROGRAM

The test program consisted of determining the effects of the various flaps on the aerodynamic characteristics of each wing alone and in combination with the fuselage. Both full-span and partial-span flaps were tested through a range of deflection angles. A secondary phase of the force tests consisted of determining the effect of various horizontal tail configurations on the static longitudinal stability of wing-fuselage combinations.

Practically all of the test runs were made through a full angle of attack range from zero through stall. Angle of attack increments varied from two degrees for basic wing runs to four and eight degrees for other configurations. Near the stall these increments were reduced sufficiently to obtain a well defined lift-curve peak.

Flow pattern studies were made on several representative model configurations by means of tufts attached to the upper surface of the wing. Photographs of the tuft action were taken at various angles of attack from zero through the stall. The angle of attack increments in each case were such that a definite change in the flow pattern could be observed from the tuft action.

All the model combinations were tested at a dynamic pressure of about 11.0 pounds per square foot. The Reynolds number based on the mean aerodynamic chord and a dynamic pressure of 11.0 pounds per square foot was approximately 390,000 for both wings.

IV. DISCUSSION OF CORRECTIONS

Since the primary objective of this research was to determine the relative effects of the fuselage and the various high-lift devices on the basic wing characteristics, no corrections were made for tunnel wall effects on either the induced drag or the induced angle of attack. The resistance of the model supports was arbitrarily accounted for by reducing all the drag results by a factor of $C_{D_t} = 0.010$ (Cf. Ref. 1); however, no corrections were made for the aerodynamic interference effects between the model and the supports.

The tests on the basic wings and the basic wing-fuselage configurations (Cf. Figs. 7 and 8) show that zero lift occurred at a positive angle of attack of about one degree, rather than at zero angle of attack as would be expected for symmetrical airfoils. The zero lift angles for the wings tested in Ref. 1 were in error to the same order of magnitude. Part of this error is due to a twenty-minute downward inclination of the flow at the test section of the tunnel as indicated by previous experiments. The remainder of the error may possibly be due to curvature of the flow in the test section (Cf. Ref. 1).

The results of all the force tests were reduced to standard non-dimensional force coefficients, C_L, C_D, and $C_{M_{a.c.}}$, based on the area and the mean aerodynamic chord of the wing alone. The aerodynamic center was determined

from the average slope of the pitching moment curve near zero lift for the wing alone. It was found to be at 0.182 of the mean aerodynamic chord for the straight wing and at 0.372 of the mean aerodynamic chord for the swept-forward wing.

At angles of attack near maximum lift the trailing portions of the models approached rather close to the floor of the tunnel. This may have had some effect on the results obtained at these attitudes, particularly in the case of the fuselage with the horizontal tail.

V. DISCUSSION OF TEST RESULTS

The test results are presented as plots of C_D, α, and $C_{M_{a.c.}}$ against C_L as ordinate. These curves are shown in Figs. 7 through 31. The maximum lift coefficients for the various model configurations tested are summarized in Figs. 32 and 33. In connection with these summary curves it can be observed that the straight wing configurations gave higher maximum lifts than were obtained with the sweptforward wing configurations, and that the optimum flap deflection is better defined. Tuft pictures showing the stall pattern of representative model combinations are shown in Figs. 34 through 46.

Fig. 7 is a comparison of the characteristics of the two basic wings. The effects of wing-planform shape are clearly evident from the differences indicated on the lift and moment curves. Comparison of Fig. 7 with the basic wing results from Ref. 1 demonstrates wing-planform effects further. The lift curve slopes* for the sweptback and the delta wing of Ref. 1 practically match that of the straight wing. However, the maximum lift coefficients of the delta and sweptback wings are appreciably higher and occur at a

*The discussion which follows will make frequent reference to the lift curve slope, $dC_L/d\alpha$, and to the slope of the pitching moment curve, $dC_{M_{a.c.}}/dC_L$. When such reference is made, it applies to the angle of attack range over which the lift curve may be approximated by a straight line.

higher angle of attack. The effects of a change in the wing planform are also evident from a comparison of the moment curves shown in Fig. 7 and those reported in Ref. 1.

The results of the wing-fuselage tests are presented in Fig. 8. A comparison of these results with those of the basic wings (Cf. Fig. 7) shows the following changes in aerodynamic characteristics: The maximum lift coefficient is increased by about 0.26; the angle of attack corresponding to this lift coefficient is increased for both combinations; the lift curve slope is increased by a small amount; and, the slope of the moment curve is increased in the positive sense. Changes in the shape of the lift curve peak are also evident, with the greater change occurring on the straight wing combination. In contrast, results from Ref. 1 show that the sweptback wing-fuselage combination had an incremental maximum lift coefficient of 0.12, whereas the delta wing combined with the same body showed a decrease in maximum lift of 0.12. No significant changes in either the shape of the lift curve peak or the angle of attack corresponding to maximum lift were observed for the wing-fuselage combinations tested in Ref. 1.

The results of the tests on the wing-fuselage-tail combinations are shown in Figs. 9 and 10. The horizontal tail tends to increase the static longitudinal stability of the configuration with the sweptforward wing (Cf. Fig. 9),

although the amount by which the slope of the moment curve is changed is a function of tail location and tail sweep angle. The fact that the sweptback tail-high configuration is more stable than the sweptforward tail-high combination can be attributed to two causes; a) in the sweptback configuration the effective tail length is greater, and b) the sweptback tail has a greater lift curve slope than the sweptforward tail (Cf. Fig. 7 and Ref. 1). Change in the tail lever arm also accounts in part, at least, for the fact that the tail-high configuration is more stable than the tail-low configuration. The moment curves in Fig. 10 for the straight wing-fuselage-tail combination indicate horizontal tail effects which are not in total agreement with those observed in Fig. 9. Part of the difference may be attributed to variation in downwash and downwash distribution behind the two wings. Fig. 10 also shows the effect of the conical nose on the straight wing-fuselage combination. This nose piece was also tested on the fuselage combined with the sweptforward wing with no measureable change in the characteristics from those observed with the ducted fuselage.

The effects of the plain leading edge partial span flaps on the sweptforward wing are presented in Fig. 11. Although these flaps exhibit practically no effect on the magnitude of the maximum lift coefficient or the slope of the lift curve, they do exert considerable influence on the shape of the lift curve peak.

Figs. 12, 13 and 14 give the characteristics of the sweptforward wing and wing-fuselage models combined with full- and partial-span extended leading edge flaps. Although these flaps show a slight increase in the maximum lift coefficient, most of the increment can be attributed to the additional wing area resulting from flap extension. The small variation in the maximum lift may be attributed to change in the camber with flap deflection. The essential effects of these flaps are a flattening of the lift curve peak and a destabilizing effect on the model. Partial span flaps of this type show the same general effects to a reduced order of magnitude.

The characteristics of the sweptforward wing and wing-fuselage models combined with split flaps are given in Figs. 15, 16 and 17. The effects shown are typical for split flaps; i. e., an increase in the lift coefficient for a given angle of attack, an increase in the maximum lift coefficient, a shift of the moment curve to greater negative values, and a slight decrease in the slope of the moment curve. In general, reduced span and deflection produce the same effects to a lesser degree.

The results for the tests with extended trailing edge flaps on the sweptforward wing configurations are presented in Figs. 18, 19 and 20. Not only are the lift increments for any given angle of attack greater than those of the previously-mentioned devices, but the slope of the lift

curve is also increased. Hence, these flaps prove advantageous from the lift standpoint over the whole flight range of angle of attack. Some of this advantage is lost when consideration is given to the large negative pitching moments that these flaps produce at landing attitudes. Comparison of the moment curves of Figs. 18 and 19 reveals a departure from trends previously observed in this report for partial span flaps. The higher negative moments obtained with the 70 per cent span flaps may be attributed to the fact that the center of pressure has moved aft for the same lift. This is due to removal of flap area at the wing tips. The same effect is also apparent in Fig. 20 where full- and partial-span flap results are presented for the sweptforward wing-fuselage combination.

The results of the tests made on the straight wing configurations are presented in Figs. 21 through 31. The high-lift devices produced three effects on model configurations using this wing which were directly opposite to the effects observed on the sweptforward wing combinations. The first of these, and perhaps most significant, was the fact that lift increments produced by flaps were less on the straight wing-fuselage combination than they were on the wing alone. A second characteristic, also very important from the standpoint of the landing problem, was that for comparable flap type and deflection the maximum lift occurred at a lower angle of attack for the straight

wing models. In connection with this fact, it was also observed that the straight wing configurations had a greater lift curve slope than did the corresponding swept-forward wing configuration. The third effect may be observed from a comparison of the pitching moment curves near maximum lift for similar model configurations. In the case of the sweptforward wing tests it is apparent that large increases in negative pitching moments occur at attitudes near and beyond maximum lift. The tests of the straight wing show that pitching moment changes were comparatively small at lift coefficients beyond the stall.

The effects of the extended leading edge flap on the straight wing model configurations are shown in Figs. 21, 22 and 23. These flaps produced slight changes in the lift of the basic model at low angles of attack, but did improve the maximum lift somewhat by an extension of the basic curve. In the case of the wing-fuselage configuration, a sharper lift curve peak was obtained with the flaps extended (Cf. Fig. 23).

The aerodynamic characteristics of the straight wing model configurations using split flaps are given in Figs. 24 through 27. In general, the characteristics of the basic model are modified in the normal manner.

The effect of change in chord of the split flap can be observed from a comparison of Figs. 24 and 25. The maximum lift which can be obtained with the 12.5 per cent

chord flap (Cf. Fig. 25) is essentially equal to that obtained with the 25 per cent flap (Cf. Fig. 24). However, the deflection angle corresponding to optimum lift is greater for the flap with the reduced chord. In general, the same quantitative effects can be obtained with the 12.5 per cent chord flap as with the 25 per cent chord flap. This is evident when a comparison is made between the 20 degree flap curve of Fig. 24 and the 40 degree flap curve of Fig. 25.

The effects of the reduced span split flaps on the straight wing characteristics can be obtained by comparing Figs. 24 and 26. The 70 per cent span flaps have a greater lift curve slope than do the full-span. For a 20 degree deflection angle, both have the same maximum lift; at a 40 degree flap angle the partial-span flap produces the greater maximum lift. Below the stall, however, the full-span flap gives greater lift for a given flap deflection and wing angle of attack. The negative shift in the moment curve is less using partial-span flaps. The same general remarks apply to Fig. 27, which presents the results of full- and partial-span split flap tests on the straight wing-fuselage combination.

A comparison of the lift curves of Fig. 27 with that for the unflapped model (Cf. Fig. 7) shows that increased lift is obtained over the whole flight range of angle of attack, the peak of the lift curve is more pronounced,

and maximum lift is obtained at a reduced angle of attack. The increments in maximum lift are less on this model than they were for the comparable wing alone configuration. The effect of the flaps on the moment curves of the wing-fuselage combination are similar to those observed on the wing alone configuration.

Figs. 28 through 31 are plots of data obtained using extended trailing edge flaps on the straight wing configuration. The powerful effects of these flaps on the basic model characteristics are immediately apparent. An evaluation of these effects indicates that they arise from a combination of geometric modifications on the wing brought about by flap extension. These modifications may be summarized briefly as a change in camber of the airfoil section and a decrease in the aspect ratio of the wing.

An analysis of the test results obtained for the extended trailing edge flaps shows that they are extremely effective as a high-lift device. Unfortunately, the large lift increments are accompanied by exceedingly high negative pitching moments. The angle of attack for maximum lift decreases with increase in flap deflection and may be greater than or less than that of the basic model. The drop in lift after the maximum has been attained is, in general, quite abrupt, especially for the straight wing alone with partial span flaps (Cf. Fig. 30).

The tests of the extended trailing edge flaps on the wing alone (Cf. Figs. 28, 29 and 30) show that for a given value of the lift coefficient a greater angle of attack is required for the 70 per cent span flaps at a given deflection than for the full-span flaps at the same deflection. The stall is delayed to a higher angle of attack for the reduced span, and a greater maximum lift coefficient is obtained. The same remarks apply to the wing-fuselage combination, except that the maximum lift was less for the reduced span flap (Cf. Fig. 31).

From an overall consideration of the results obtained in this investigation, it is apparent that the split and the extended trailing edge flaps show reasonable promise as high-lift devices for wings of the type tested. It is also apparent that further research on these devices is desirable in order to obtain more conclusive data on the effect of changing the flap and the wing parameters. The results of the tests reported also suggest that combinations of various leading and trailing edge devices may prove effective. Due to limitations of the equipment available, no attempt was made to evaluate the effect of Reynolds number on the aerodynamic characteristics of the models tested. Where quantitative results are desired, it is recommended that they be obtained closer to the range of flight Reynolds numbers.

VI. CONCLUSIONS

The following conclusions can be made from the results of this investigation:

1. The combination of the fuselage and the sweptforward or the straight wing had a higher maximum lift coefficient than the corresponding basic wing alone.

2. The slope of the lift curve was greater for a given straight wing model configuration than that obtained for the comparable sweptforward wing model.

3. In general, the high-lift devices were more effective on the straight wing than on the sweptforward wing.

4. For comparable flap span and deflection the maximum lift coefficients obtained with the high-lift devices on the straight wing alone were greater than those obtained with the same wing combined with the fuselage.

5. The increments in maximum lift obtained for a given flap configuration were approximately the same on the sweptforward wing alone as those obtained on the wing-fuselage combination.

6. The extended leading edge flaps were effective principally in modifying the lift curve peak, increasing the slope of the pitching moment curve, and shifting it toward higher positive values.

7. For a given flap span and deflection, the extended trailing edge flaps gave a greater increase in the lift than the split type.

8. For a given lift coefficient the increase in negative pitching moment was greater for the extended trailing edge flap than for the comparable split flap.

9. Partial-span split flaps and extended trailing edge flaps produced a higher maximum lift at optimum deflection on the straight wing than did the comparable full span flap. On the straight wing-fuselage combination this was observed in the split flap tests only.

10. Curves of the flap deflection plotted against the maximum lift coefficient indicated that the optimum lift was more critical with respect to the flap deflection for the straight wing than it was for the sweptforward wing.

REFERENCES

1. Jensen, Arnold A. and Koerner, Warren G.: Wind Tunnel Investigation Of A Tailless Airplane At Low Subsonic Speed. Thesis, California Institute of Technology (1948)

2. Dore, Frank: The Design Of Tailless Airplanes. Thesis, California Institute of Technology (1947)

INDEX OF FIGURES

	Figure Number
Tuft Studies	
W	34, 35
WB_1V	36, 37
W_s	38, 39
W_sB_1V	40
W_sF_3[40]	41
WF_8[40]	42, 43
$WF_8(70)$[40]	44, 45, 46

CODE OF MODEL CONFIGURATIONS

The number in the parenthesis following the flap designation refers to the portion of the wing span in per cent over which the flap extends. Omission of the number designates full-span flaps. In all cases, except F_1, partial-span flaps extended over the inboard portion of the wing. On the wing-fuselage combinations the flaps terminated at the fuselage; the per cent span notation assumes that the flap extends through the fuselage. The superscript on the flap configuration indicates the angular displacement of the flap in degrees as shown in Fig. 6. Thus $F_2(70)^{40}$ corresponds to the 70 per cent span 25 per cent chord split flap on W_s deflected 40 degrees.

W_s Basic sweptforward wing

W Basic unswept wing

B_1 Circular fuselage with full length air duct

B_2 Circular fuselage with solid conical nose piece

V Vertical sweptback tail, area = 9.83 sq. in., sweep angle = 65 degrees, aspect ratio = 0.64, taper ratio = 0.63

H_1 Horizontal sweptback tail, area = 18.2 sq. in., sweep angle = 65 degrees, aspect ratio = 1.50, taper ratio = 0.74, mounted on "V" 1.84 inches above the fuselage axis

H_2 Same as H_1 except mounted on "V" 3.68 inches above the fuselage axis

H_3 Same as H_2 except sweptforward, sweep angle = 60 degrees

F_1 Plain partial-span leading edge flaps located at the wing tip on W_s, 34 per cent span, 25 per cent chord

F_2 Split flap used on W_s, 25 per cent chord

F_3 Extended trailing edge flap used on W_s, 30 per cent chord

F_4 Split flap used on W_sB_1V, 25 per cent chord

F_5 Extended trailing edge flap used on W_sB_1V, 30 per cent chord

F_6 Split flap used on W, 25 per cent chord

F_7 Split flap used on W, 12.5 per cent chord

F_8 Extended trailing edge flap used on W, 30 per cent chord

F_9 Extended trailing edge flap used on W, 15 per cent chord

F_{10} Split flap used on WB_1V, 25 per cent chord

F_{11} Extended trailing edge flap used on WB_1V, 30 per cent chord

K_1 Extended leading edge flap used on W_s, 10 per cent chord

K_2 Extended leading edge flap used on W_sB_1V, 10 per cent chord

K_3 Extended leading edge flap used on W, 10 per cent chord

K_4 Extended leading edge flap used on WB_1V, 10 per cent chord

FIG. 1 SWEPTFORWARD WING

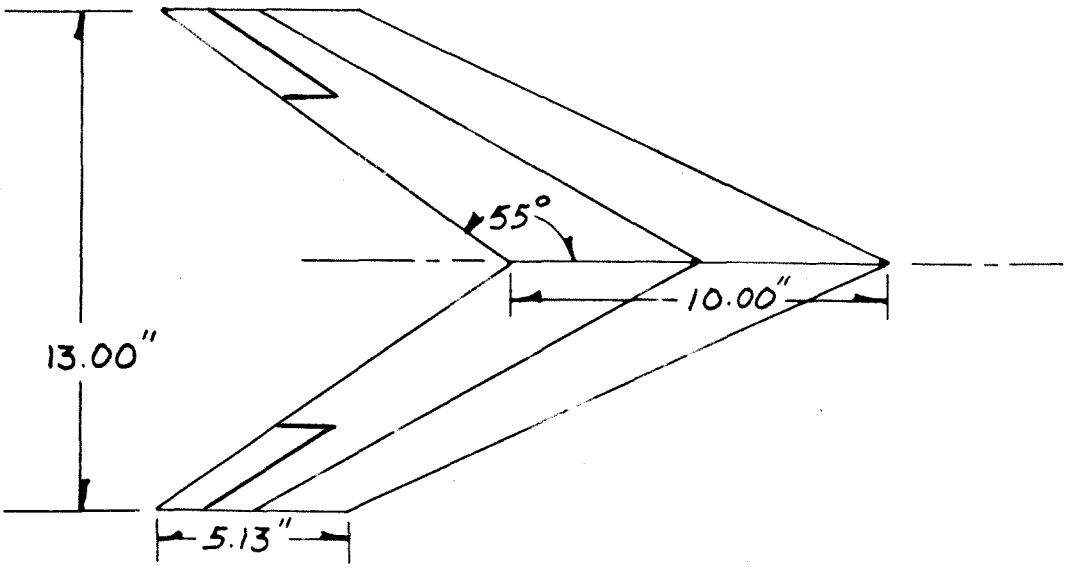

Root Chord: 5% thickness symmetrical double wedge section; maximum thickness located at .5 chord.
Tip Chord: 2% thickness symmetrical double wedge section.

FIG. 2 UNSWEPT WING

Root Chord: 5% thickness symmetrical double wedge section.

Tip Chord: 2% thickness symmetrical double wedge section.

Maximum thickness located at .5 chord.

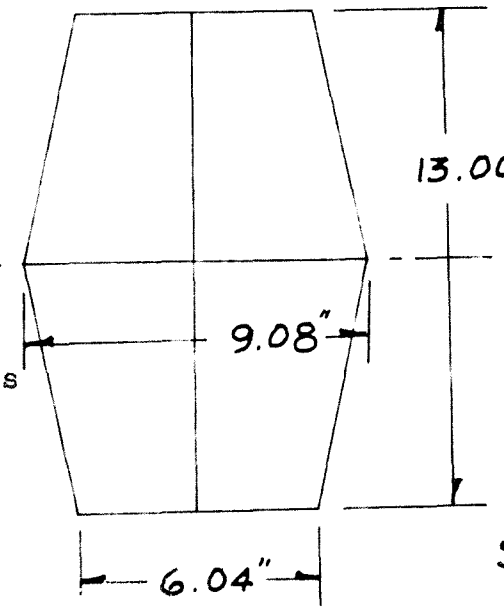

SCALE: $\frac{1}{5}" = 1"$

FIG. 3

SWEPTFORWARD WING AND FUSELAGE

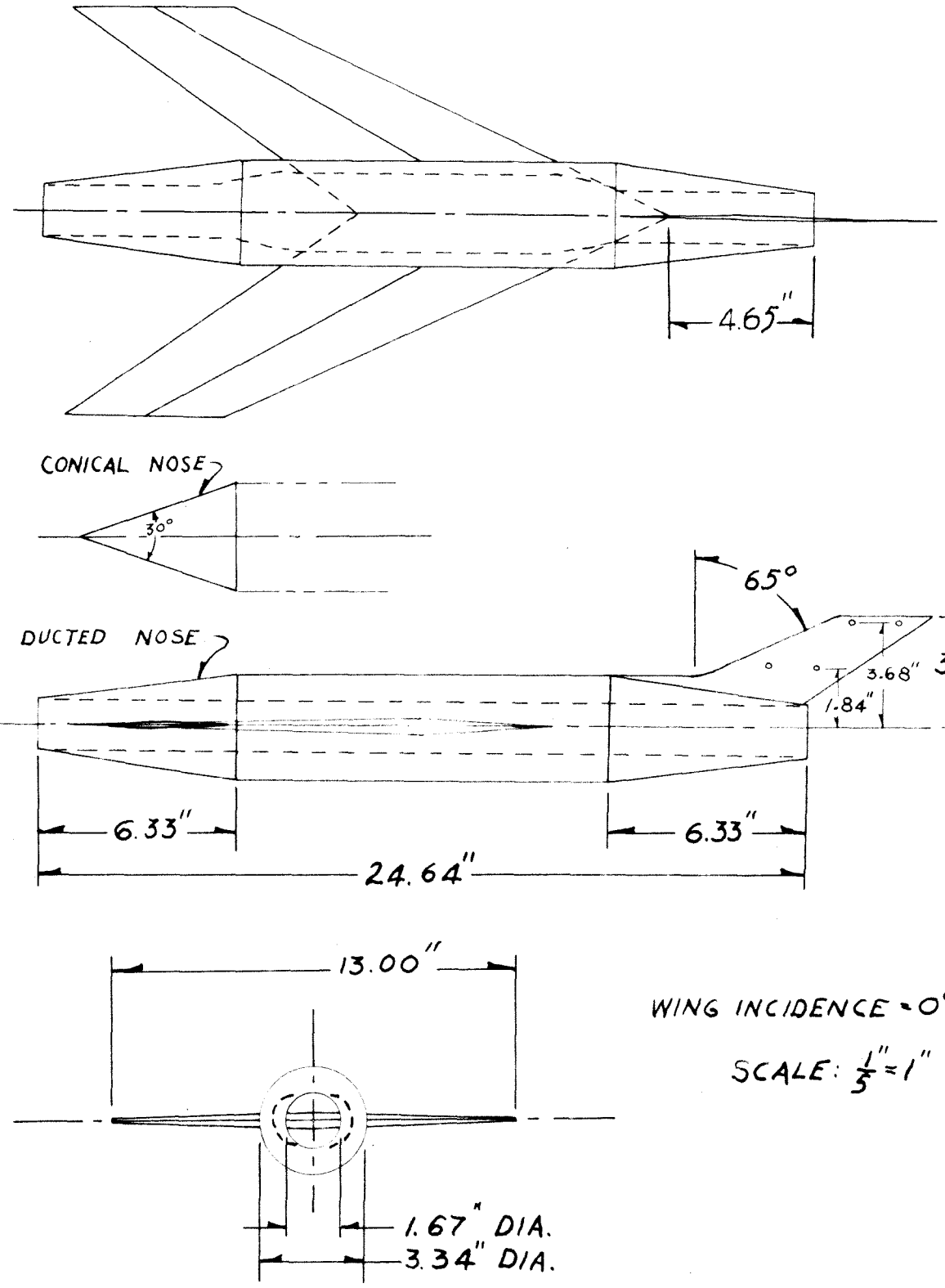

WING INCIDENCE = 0°

SCALE: $\frac{1}{3}'' = 1''$

FIG. 4 UNSWEPT WING AND FUSELAGE

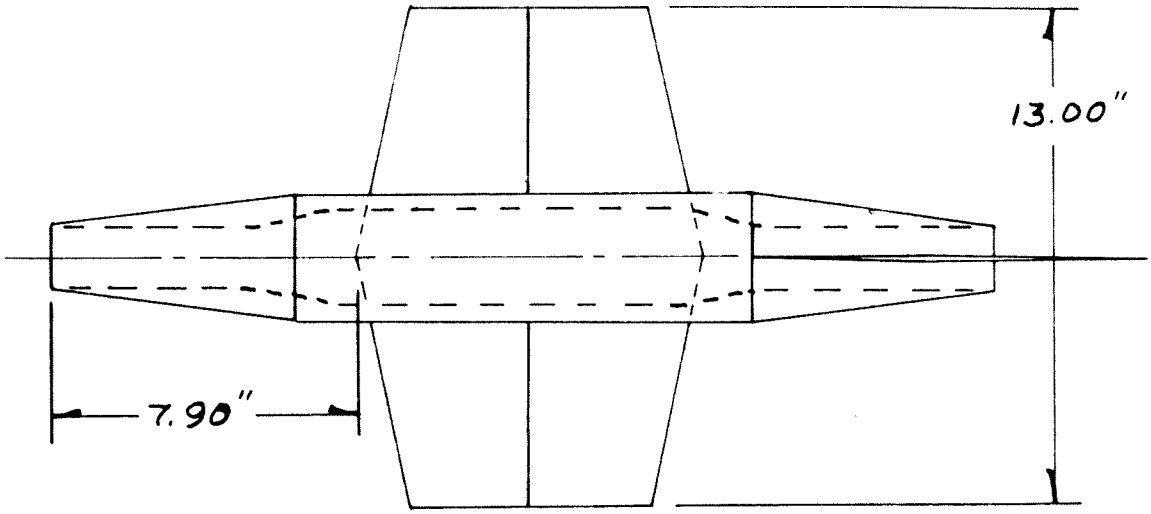

WING INCIDENCE = 0°

SCALE : $\frac{1}{5}$" = 1"

FIG. 5 HORIZONTAL TAIL

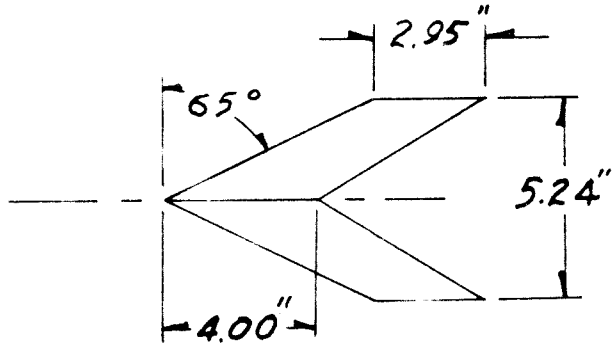

FIG. 6
FLAP ANGLES

EXTENDED LEADING EDGE FLAPS

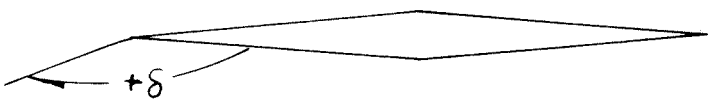

EXTENDED TRAILING EDGE FLAPS

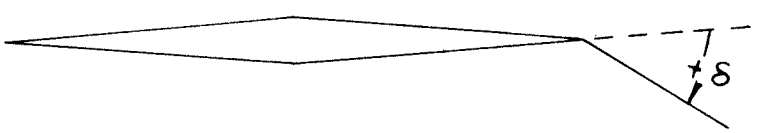

SPLIT FLAPS

PLAIN LEADING EDGE FLAPS

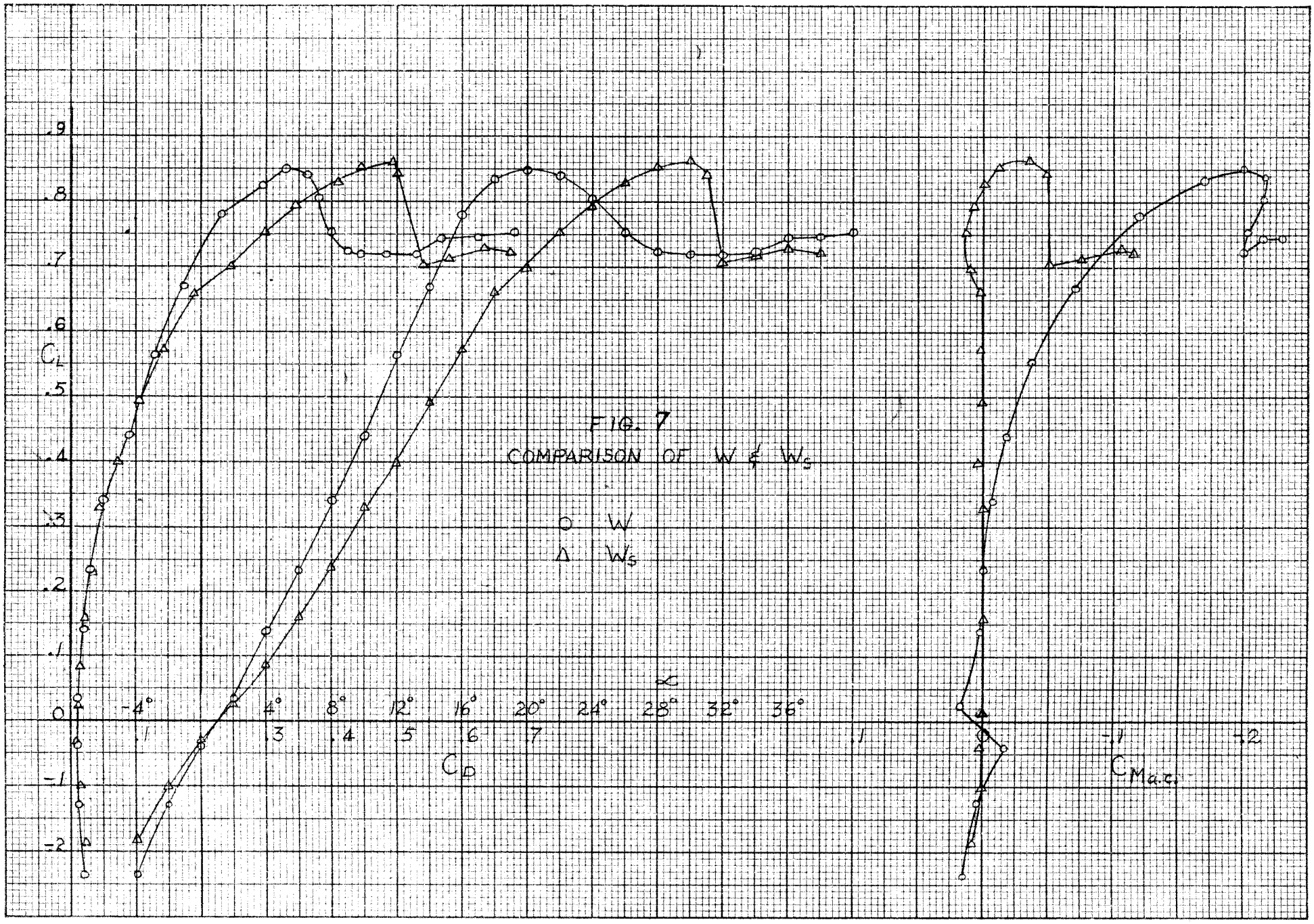

FIG. 7

COMPARISON OF W & W_s

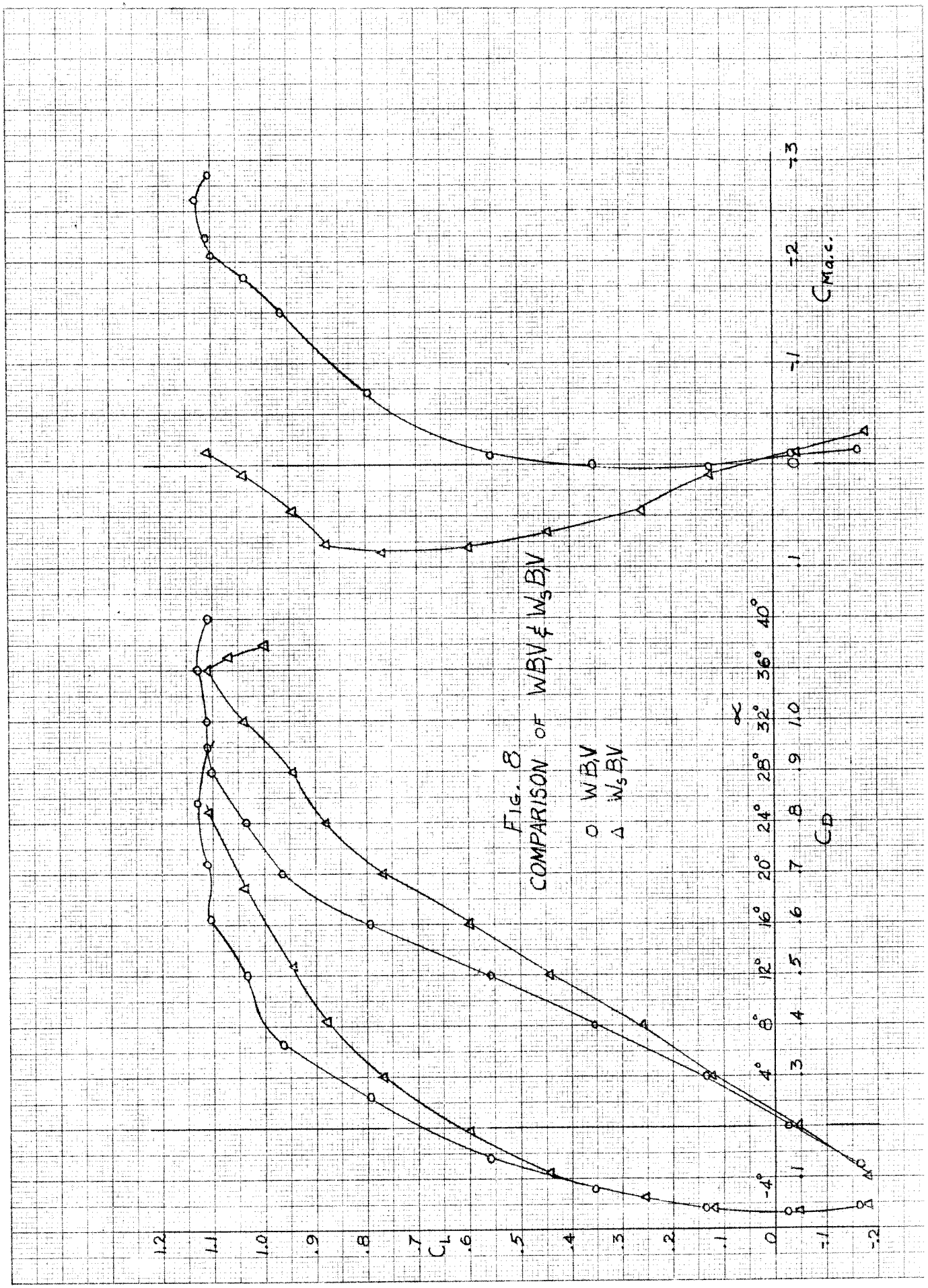
FIG. 8
COMPARISON OF WBV & WSBV
○ WBV
△ WSBV
C_L
C_D
$C_{Ma.c.}$
α
-4°
0
4°
8°
12°
16°
20°
24°
28°
32°
36°
40°
-2
-1
0
.1
.2
.3
.4
.5
.6
.7
.8
.9
1.0
1.1
1.2
-3
-2
-1
0
+1
+2
+3

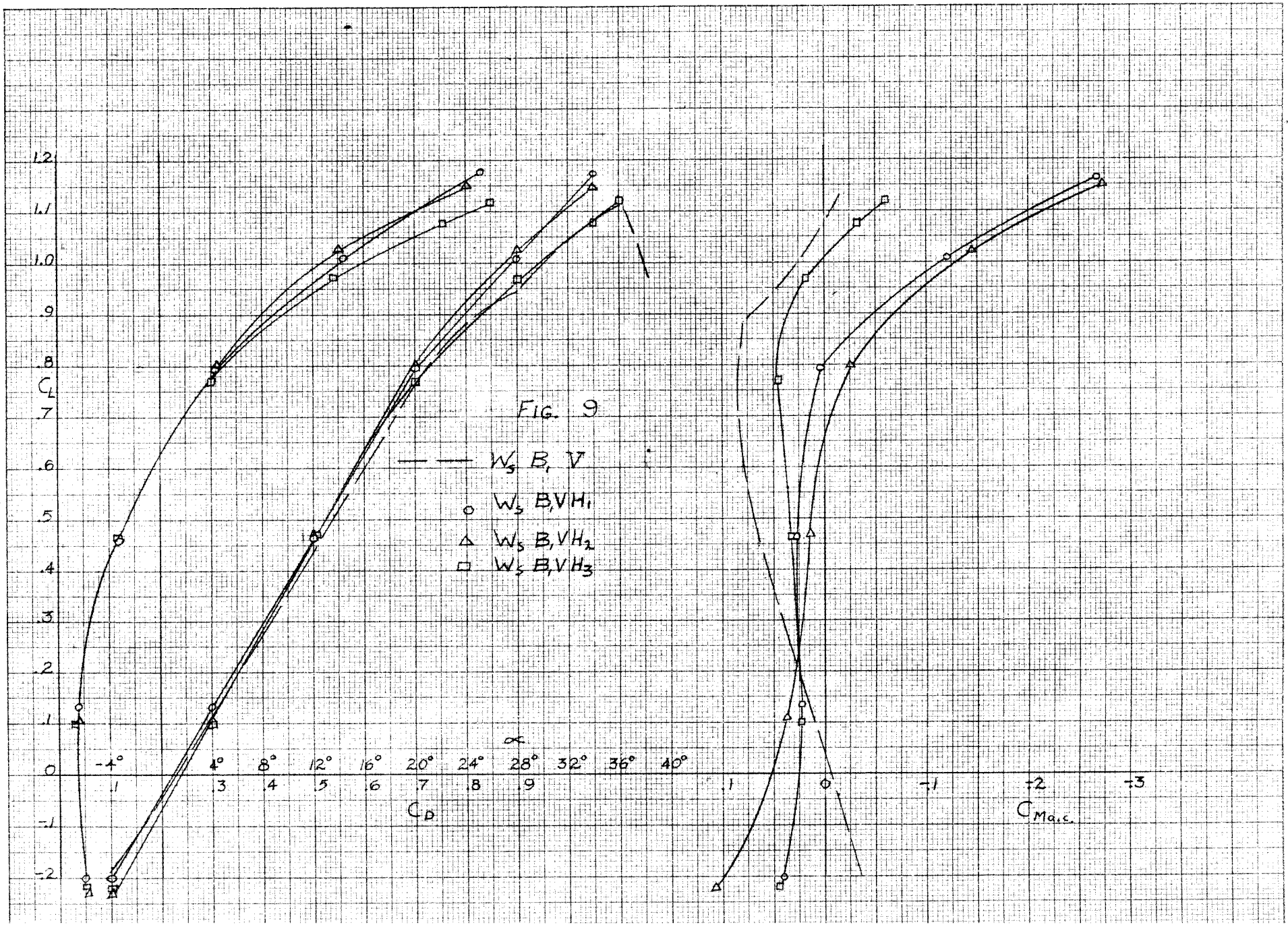
1.2
1.1
1.0
.9
.8
C_L
.7
.6
.5
.4
.3
.2
.1
0
-.1
-.2
-4°
4°
8°
12°
16°
20°
24°
28°
32°
36°
40°
α
.1
.3
.4
.5
.6
.7
.8
.9
C_D
.1
-.1
+.2
+.3
$C_{M_{a.c.}}$
W_5 B, V
W_5 B, V H_1
W_5 B, V H_2
W_5 B, V H_3

FIG. 9

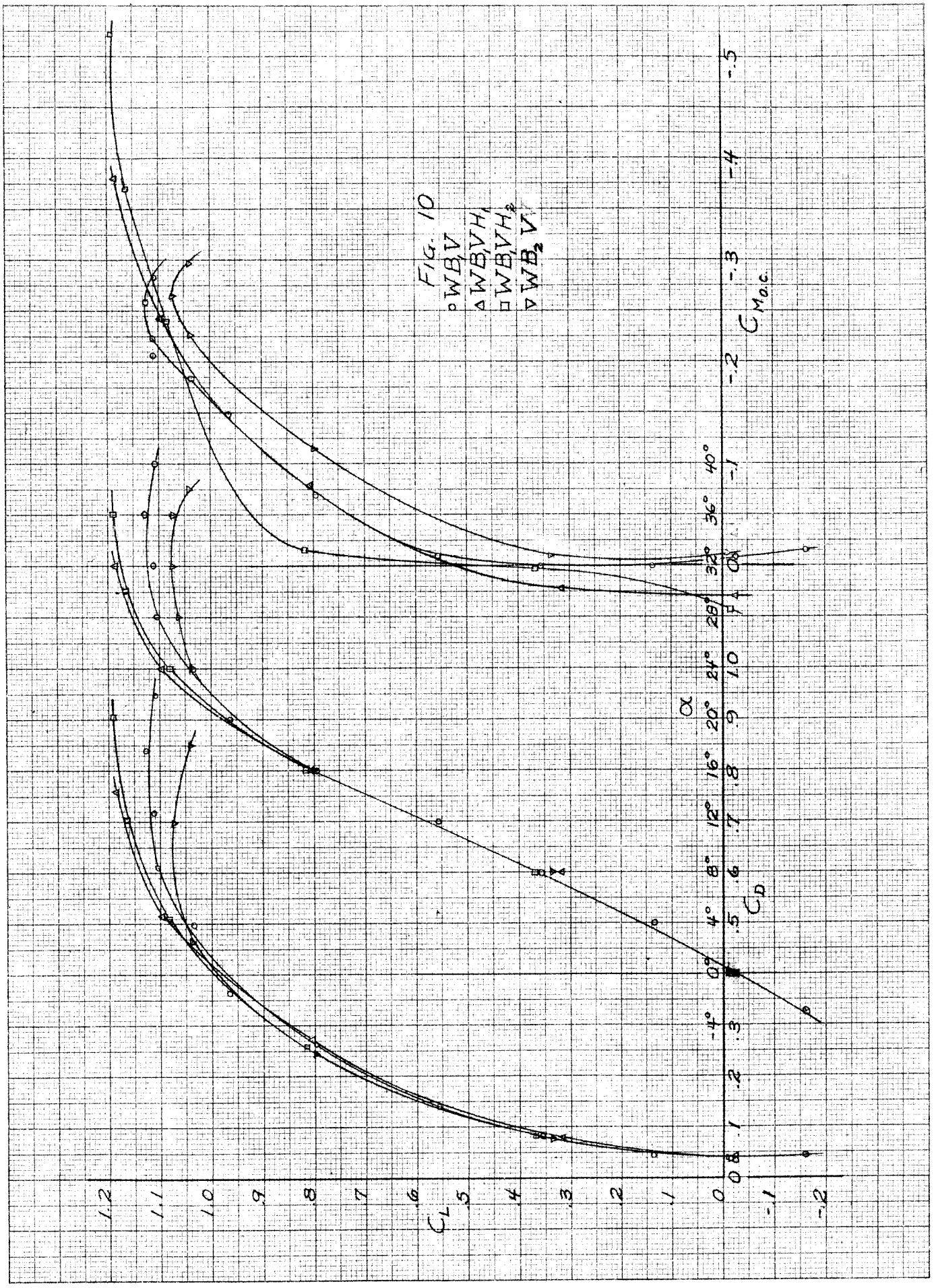
FIG. 10
○ WB, V
△ WB, VH1
□ WB VH2
▷ WB2 V
CL
CD
CM.a.c.
α
1.2
1.1
1.0
.9
.8
.7
.6
.5
.4
.3
.2
.1
0
-.1
-.2
-4°
0°
4°
8°
12°
16°
20°
24°
28°
32°
36°
40°
.5
.6
.7
.8
.9
1.0
1.1
-.5
-.4
-.3
-.2
-.1

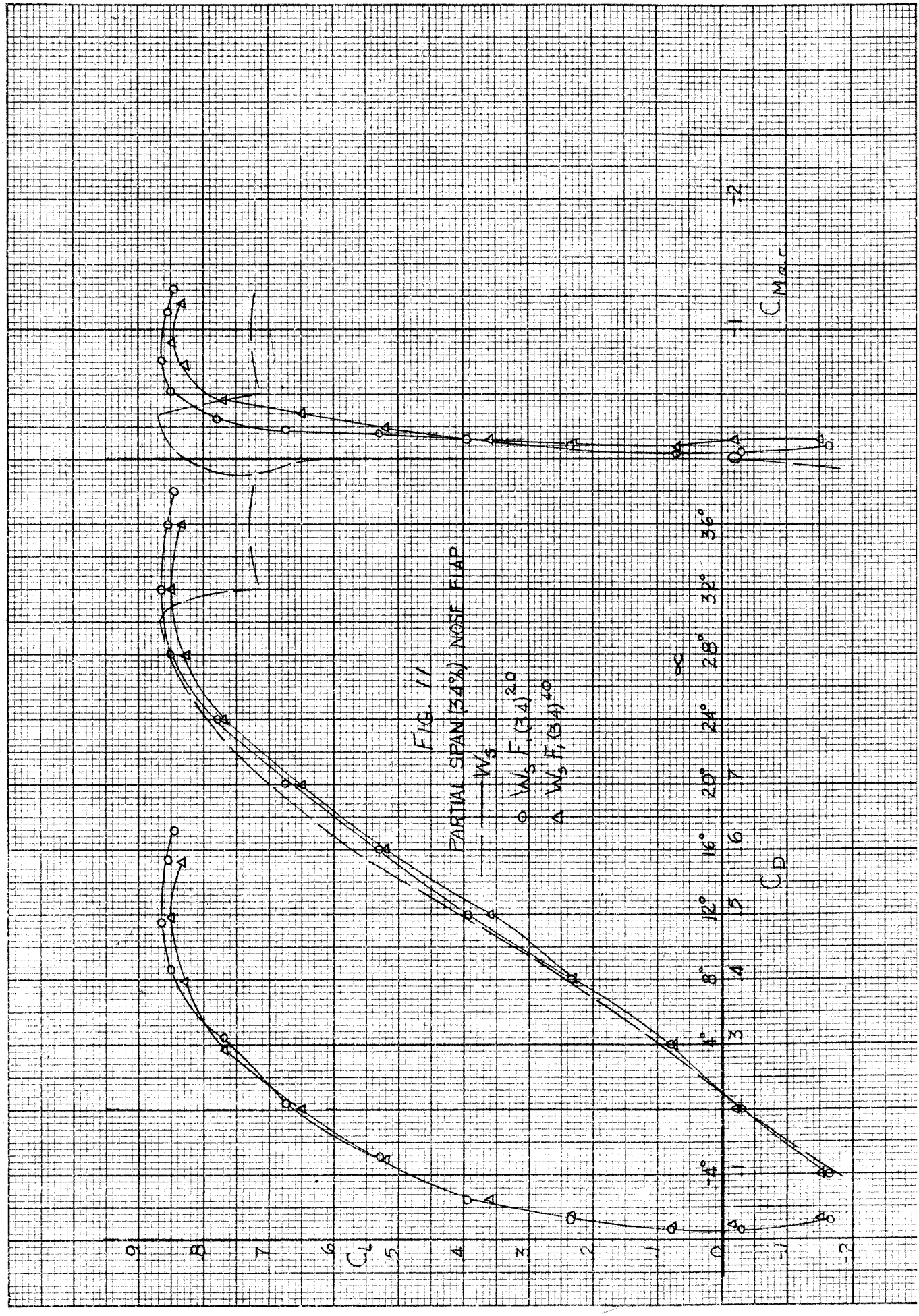
PARTIAL SPAN (34%) NOSE FLAP
$\frac{W_s}{}$
$\frac{}{}$
○ W_s F_1 (34) 20
△ W_s F_1 (34) 40
C_L
C_D
$C_{M a.c.}$
-4°
8°
12°
16°
20°
24°
28°
32°
36°

FIG. 11

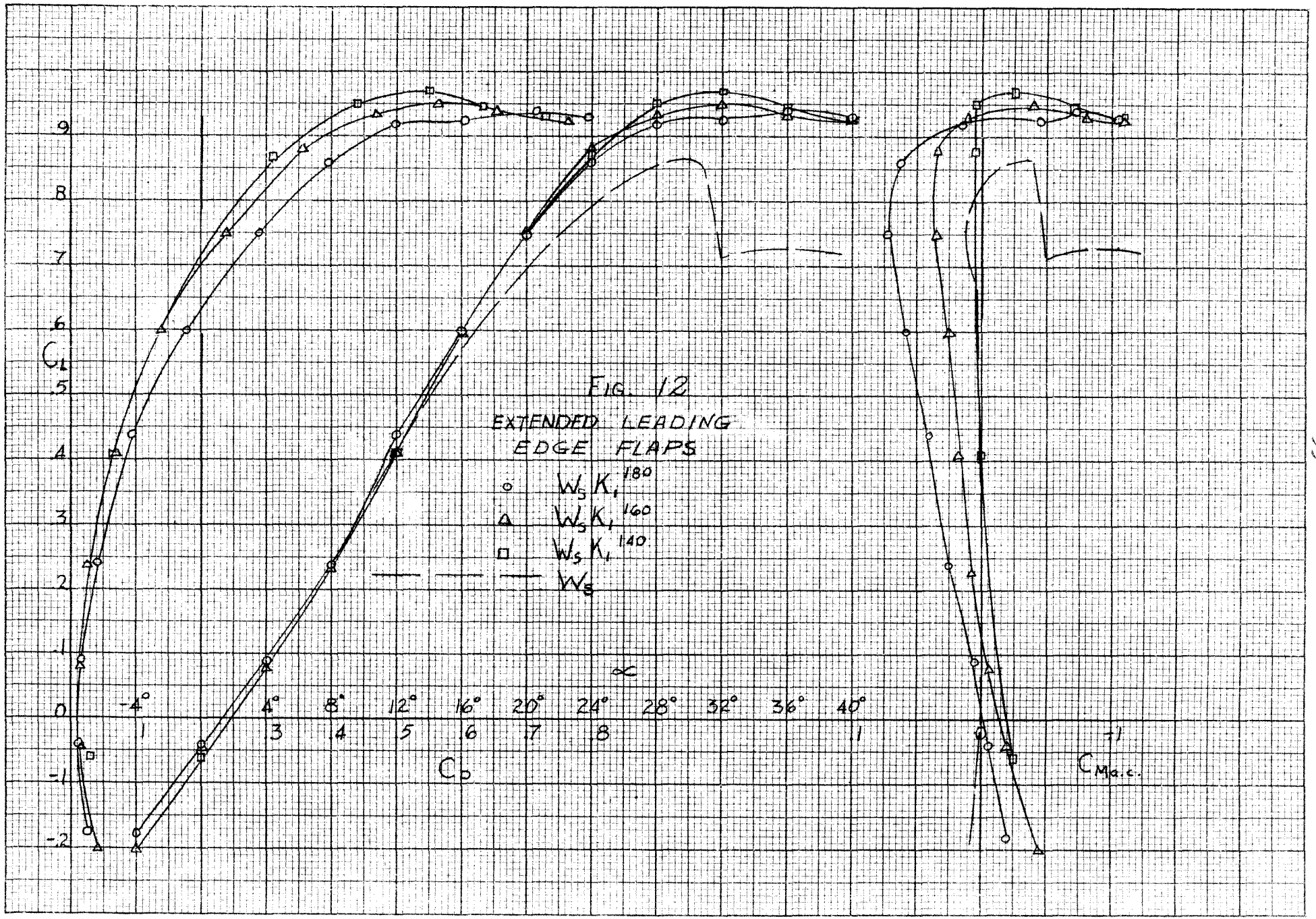
FIG. 12
EXTENDED LEADING EDGE FLAPS
$W_S K_1^{180}$
$W_S K_1^{160}$
$W_S K_1^{140}$
W_S
C_L
C_D
$C_{M a.c.}$
α
9
8
7
6
5
4
3
2
1
0
-1
-2
-4°
4°
8°
12°
16°
20°
24°
28°
32°
36°
40°
1
3
4
5
6
7
8
.1
-.1

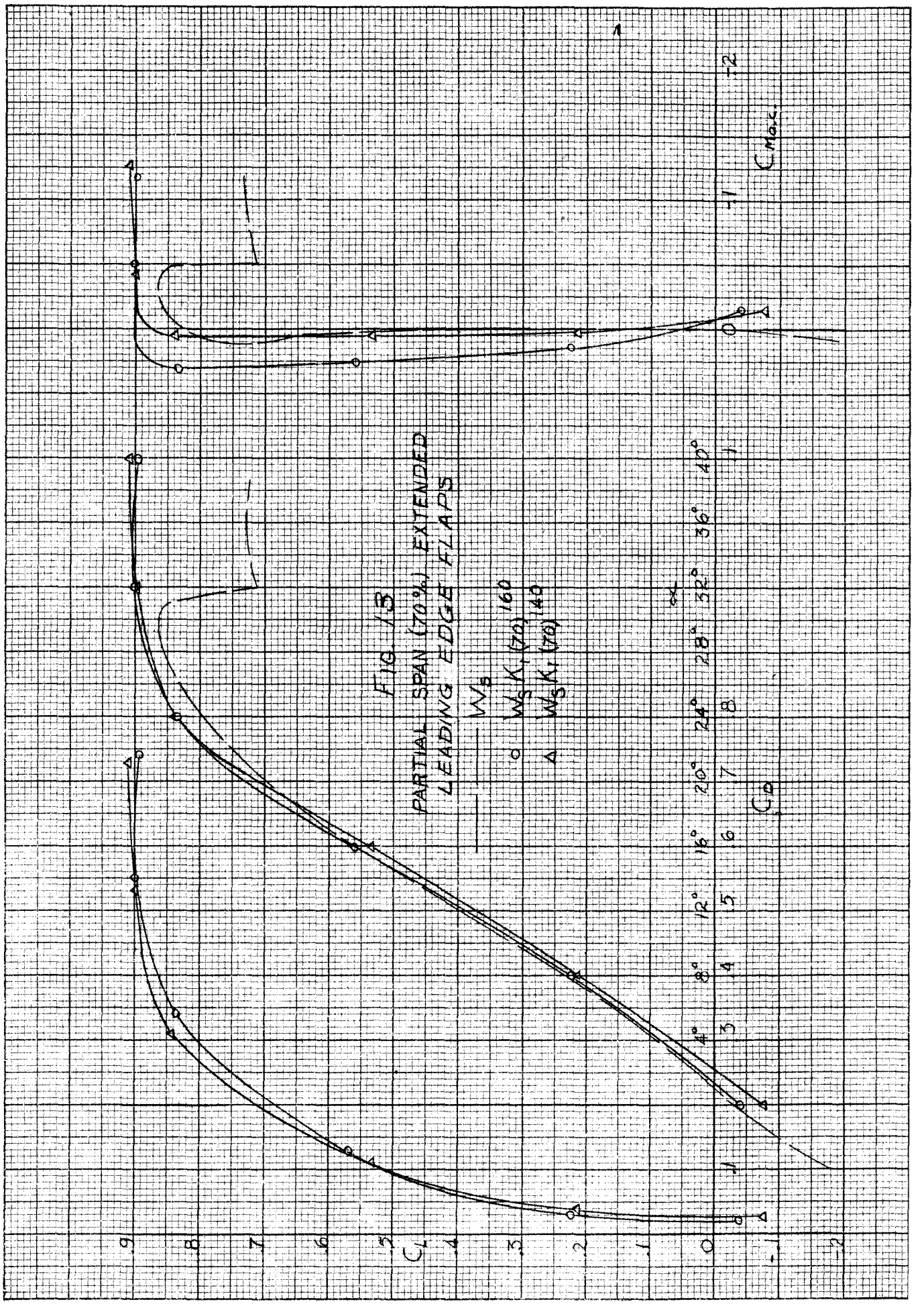
PARTIAL SPAN (70%) EXTENDED LEADING EDGE FLAPS
FIG. 15
W_S
$W_S K_1 (70)\ 160$
$W_S K_1 (70)\ 140$
C_L
C_D
$C_{M.C.}$
4°
8°
12°
16°
20°
24°
28°
32°
36°
40°

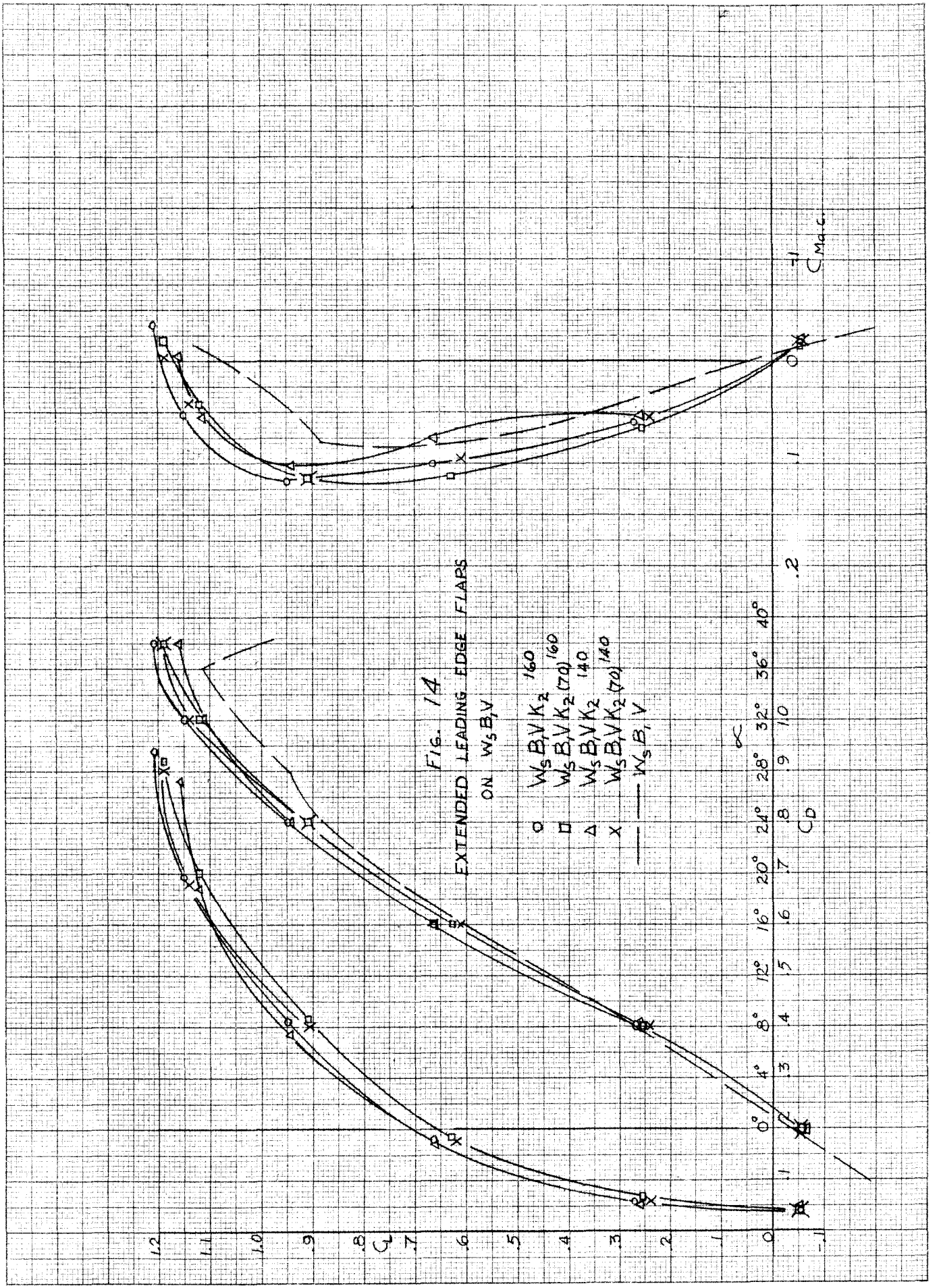
EXTENDED LEADING EDGE FLAPS
ON $W_S B, V$
$W_S B, V K_2$ 160
$W_S B, V K_2 (70)$ 160
$W_S B, V K_2$ 140
$W_S B, V K_2 (70)$ 140
$W_S B, V$
C_L
C_D
$C_{M_{a.c.}}$
α

FIG. 14

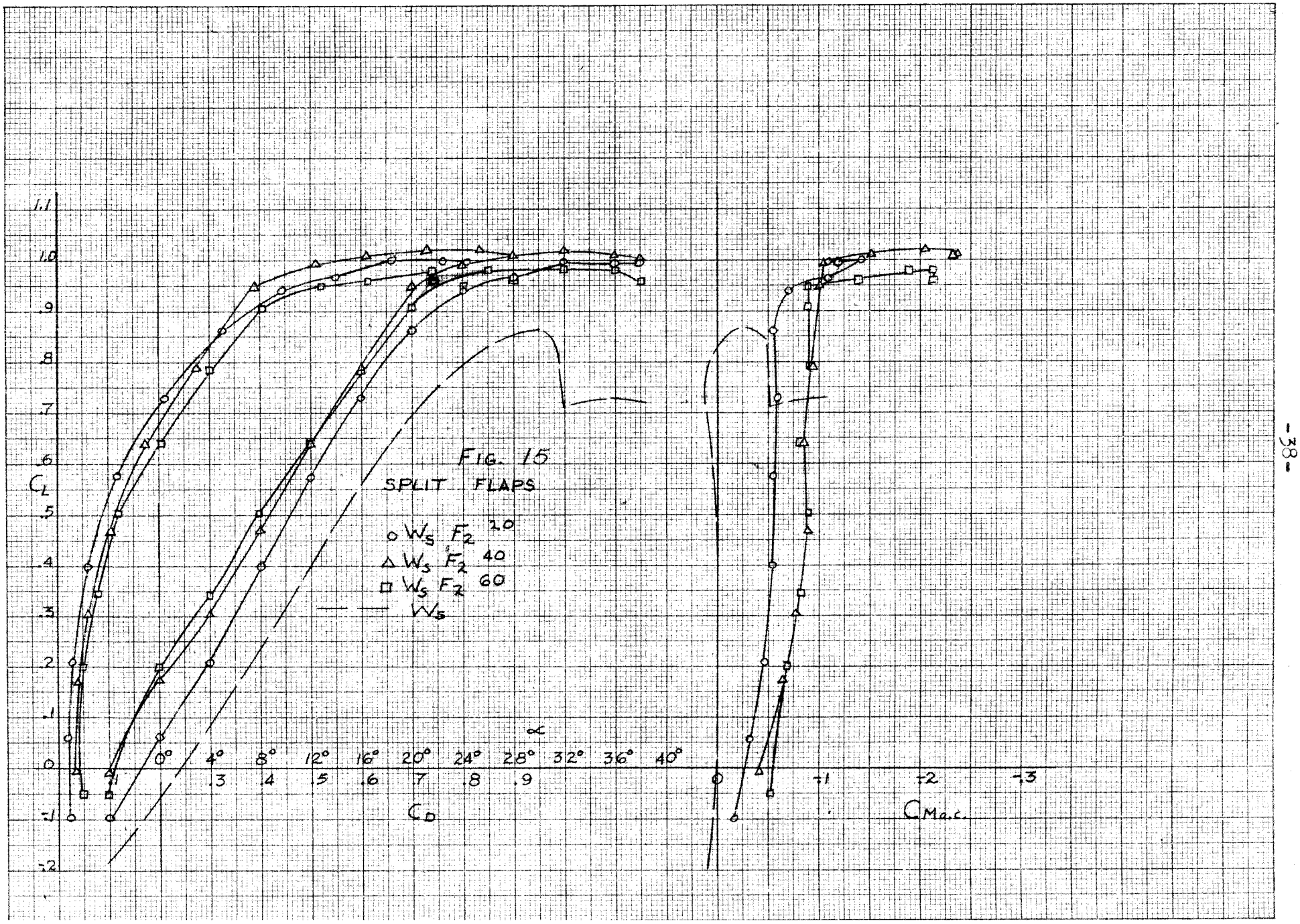
1.1
1.0
.9
.8
.7
.6
C_L
.5
.4
.3
.2
.1
0
-.1
-.2
FIG. 15
SPLIT FLAPS
○ W_s F_2 20
△ W_s F_2 40
□ W_s F_2 60
—— W_s
α
0° 4° 8° 12° 16° 20° 24° 28° 32° 36° 40°
.1 .3 .4 .5 .6 .7 .8 .9
C_D
0 +.1 +.2 -.3
$C_{M a.c.}$

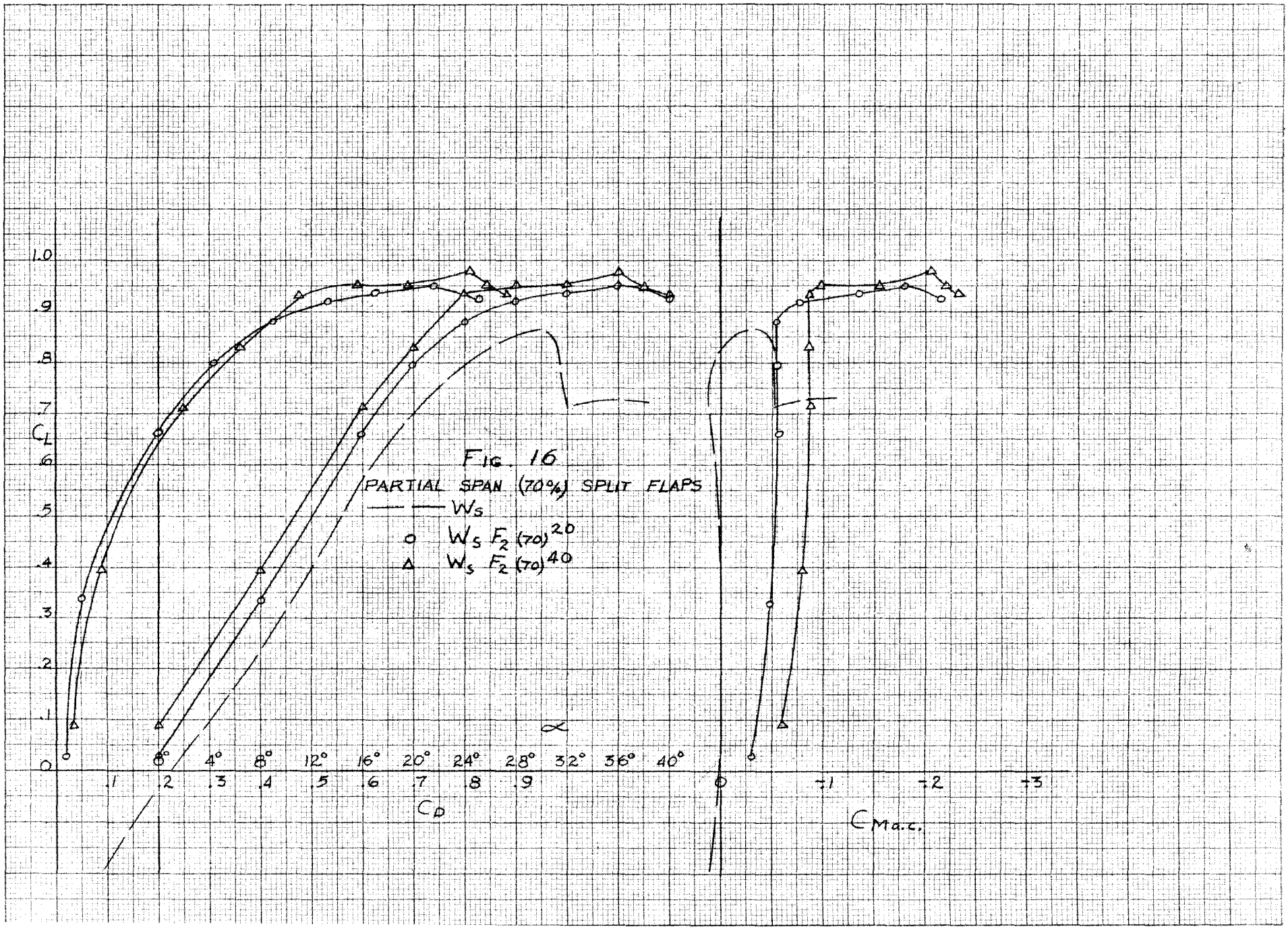
1.0
.9
.8
.7
.6
.5
.4
.3
.2
.1
0
C_L
α
0°
4°
8°
12°
16°
20°
24°
28°
32°
36°
40°
.1
.2
.3
.4
.5
.6
.7
.8
.9
C_D
0
+.1
+.2
+.3
$C_{m.a.c.}$
FIG. 16
PARTIAL SPAN (70%) SPLIT FLAPS
—— W_S
o $W_S\ F_2\ (70)^{20}$
△ $W_S\ F_2\ (70)^{40}$

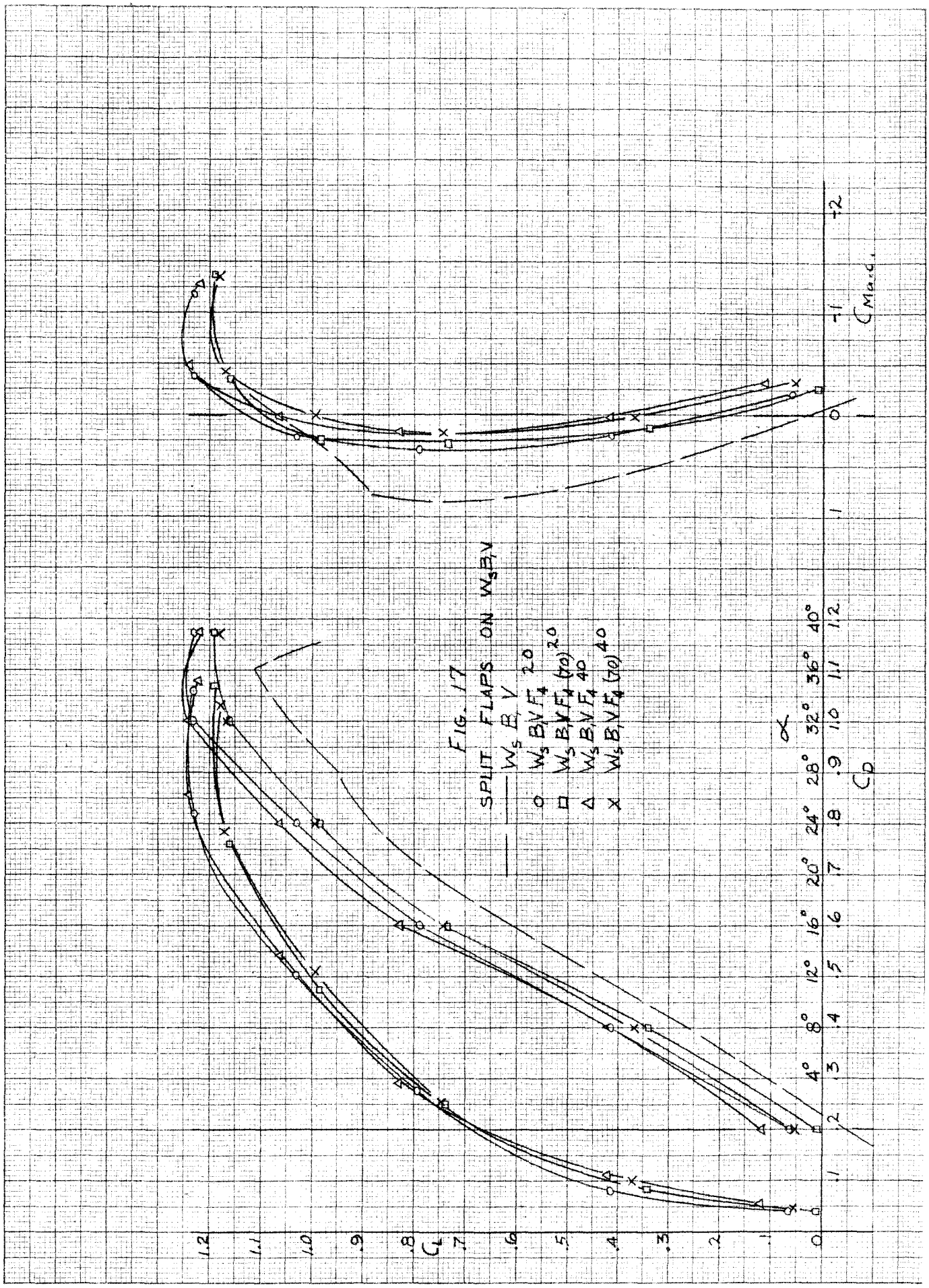
SPLIT FLAPS ON $W_S B_1 V$
$W_S B_1 V F_4$ 20
$W_S B_1 V F_4$ (70) 20
$W_S B_1 V F_4$ 40
$W_S B_1 V F_4$ (70) 40
C_L
C_D
$C_{M_{a.c.}}$
α

FIG. 17

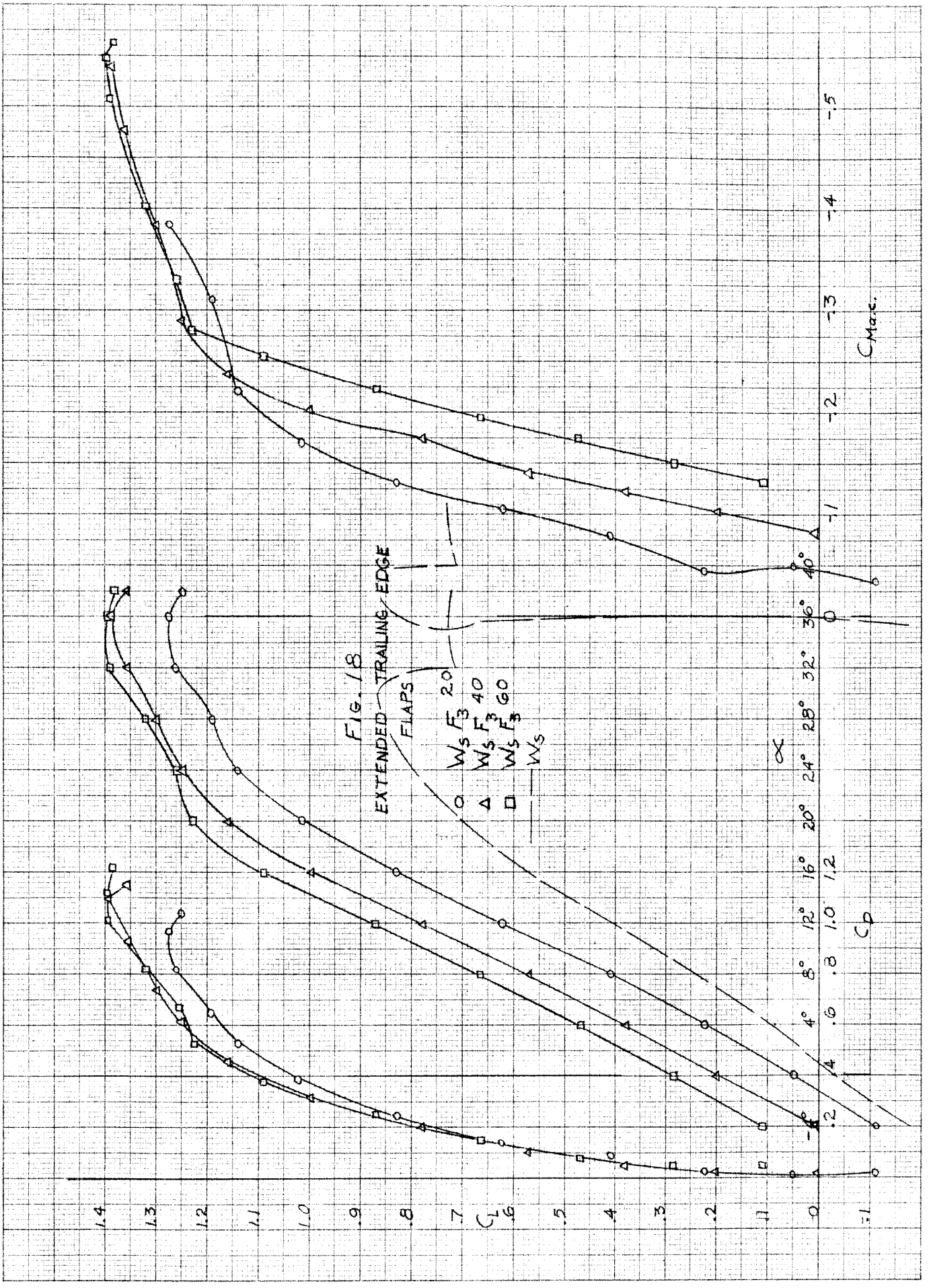
FIG. 18
EXTENDED TRAILING EDGE FLAPS
○ $W_s F_3$ 20
△ $W_s F_3$ 40
□ $W_s F_3$ 60
—— W_s
C_L
C_D
$C_{M.A.C.}$
α
L

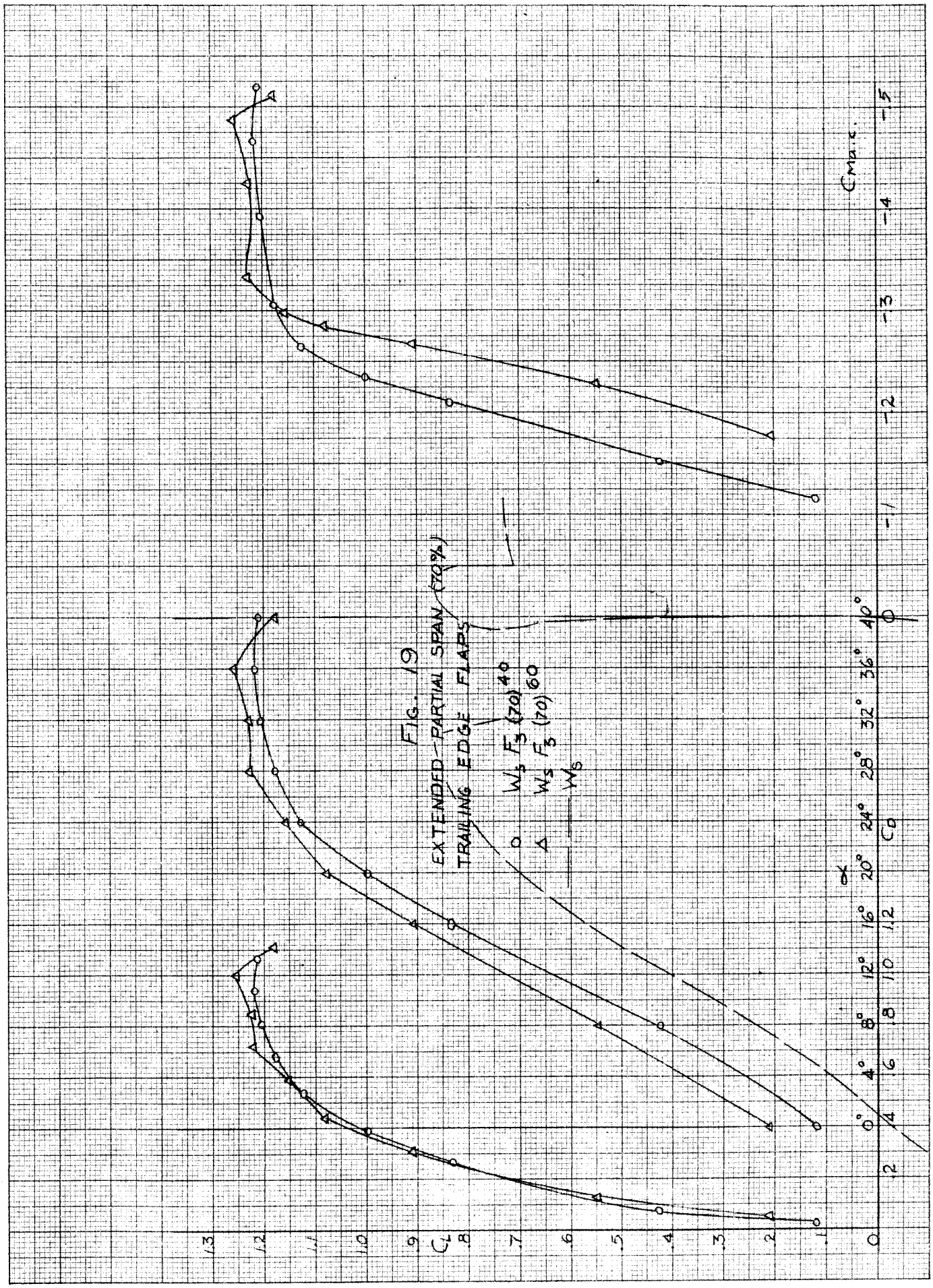
CL
CD
CMAC.
α
W/S F3 (70) 40
W/S F3 (70) 60
W/S
EXTENDED—PARTIAL SPAN (70%)
TRAILING EDGE FLAPS

FIG. 19

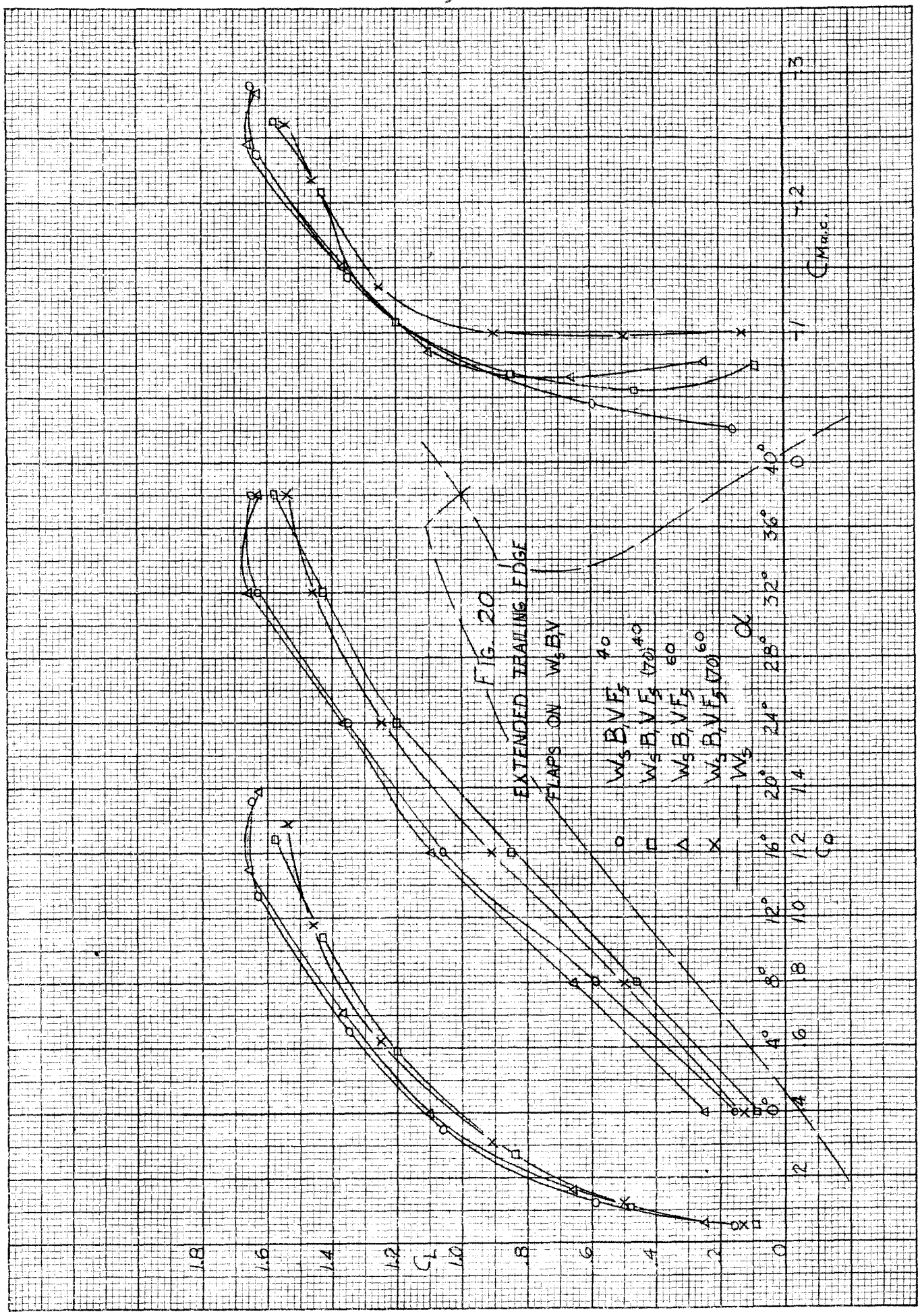
EXTENDED TRAILING EDGE
FLAPS ON $W_S B, V F_S$
$W_S B, V F_S$ (70) 40
$W_S B, V F_S$ 60
$W_S B, V F_S$ (70) 60
W_S
C_L
$C_{M_{a.c.}}$
C_D
α

FIG. 20

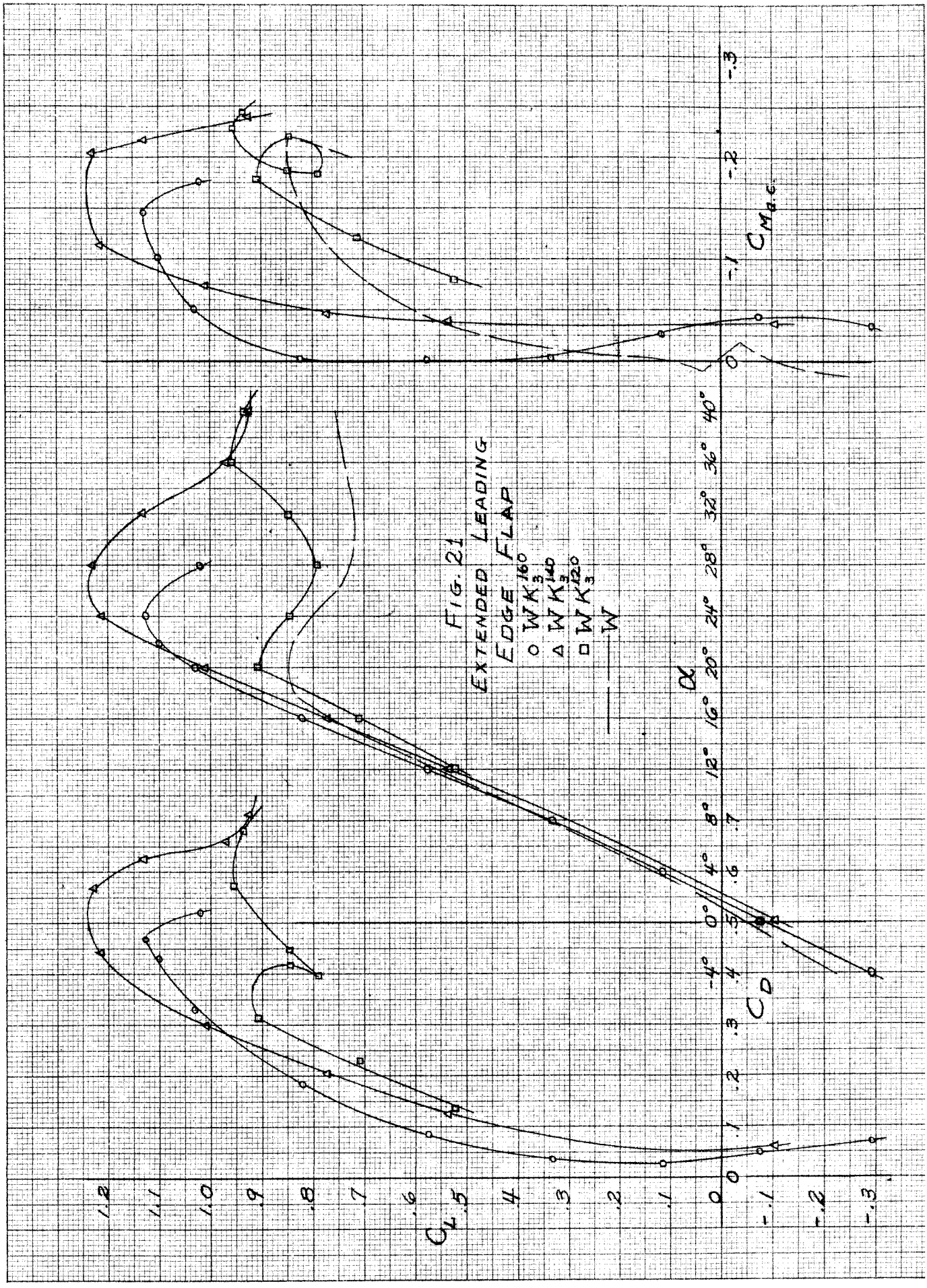
C_L
C_D
$C_{M_{a.c.}}$
α
EXTENDED LEADING EDGE FLAP
○ WK_3^{160}
△ WK_3^{140}
□ WK_3^{120}
—— W

FIG. 21

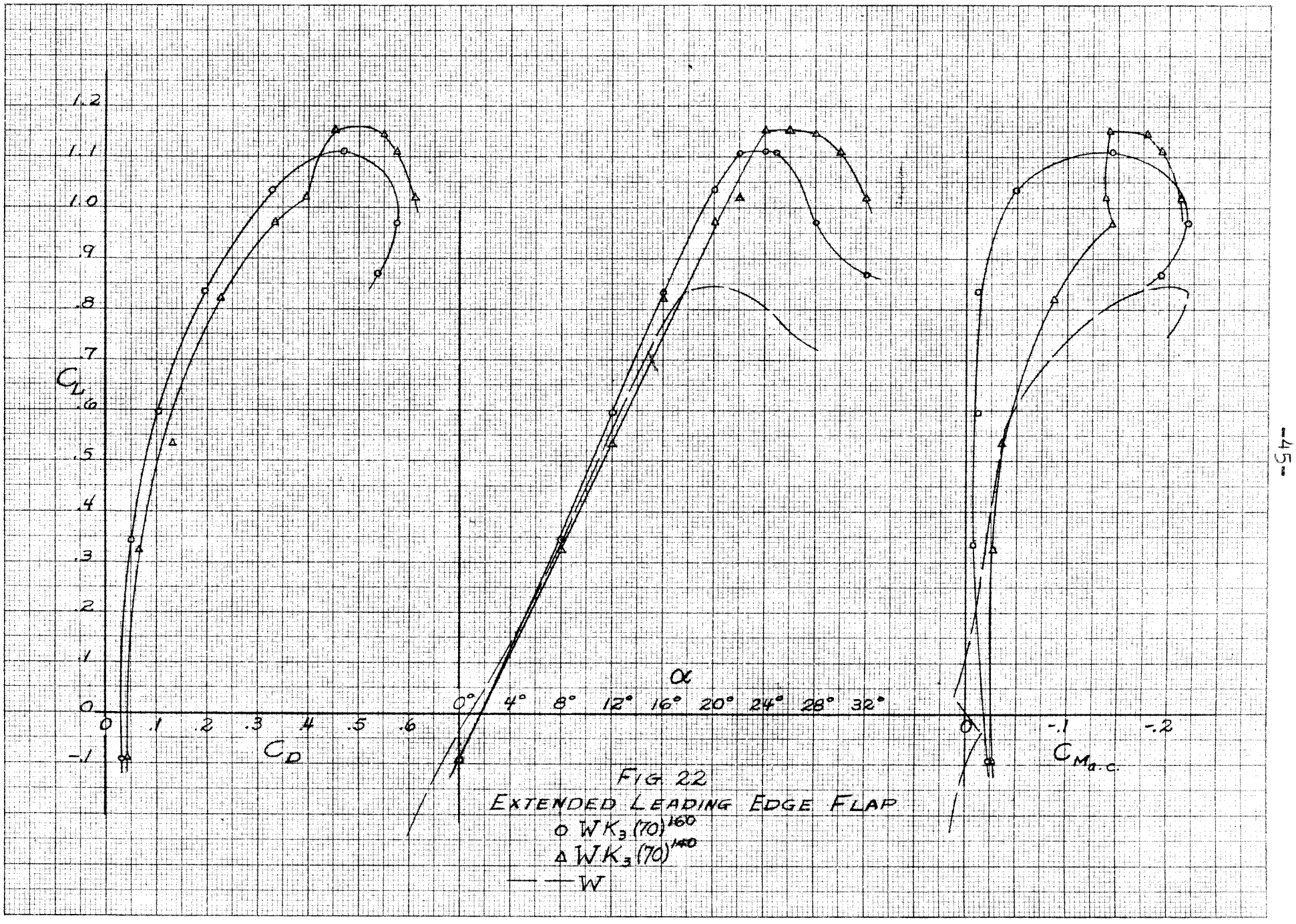

FIG 22
EXTENDED LEADING EDGE FLAP
○ $WK_3(70)^{160}$
△ $WK_3(70)^{140}$
—— W

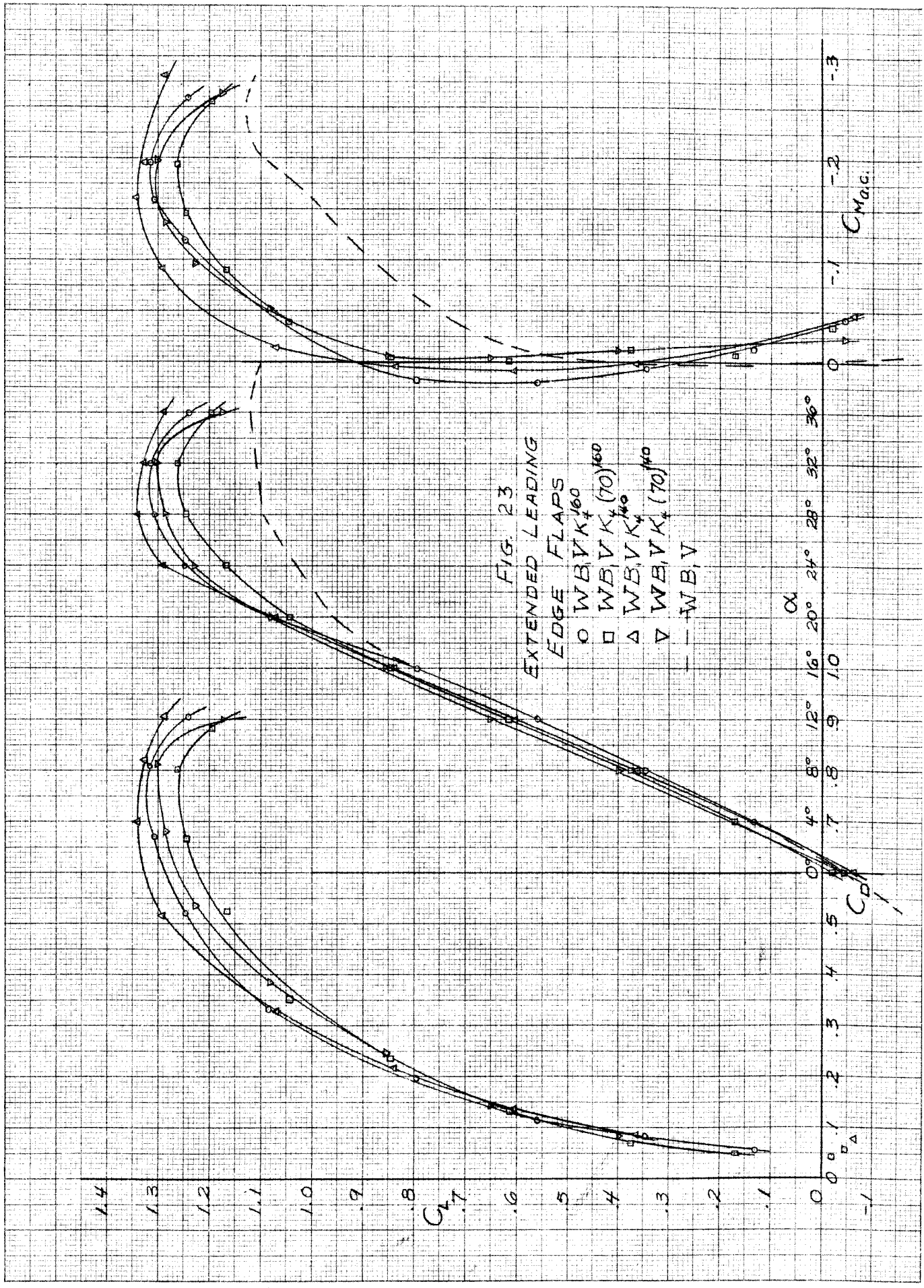
EXTENDED LEADING EDGE FLAPS
○ WBVK4 160
□ WBVK4 (70) 160
△ WBVK4 140
▽ WBVK4 (70) 140
— WBV
α
C_L
C_D
$C_{M_{a.c.}}$

FIG. 23

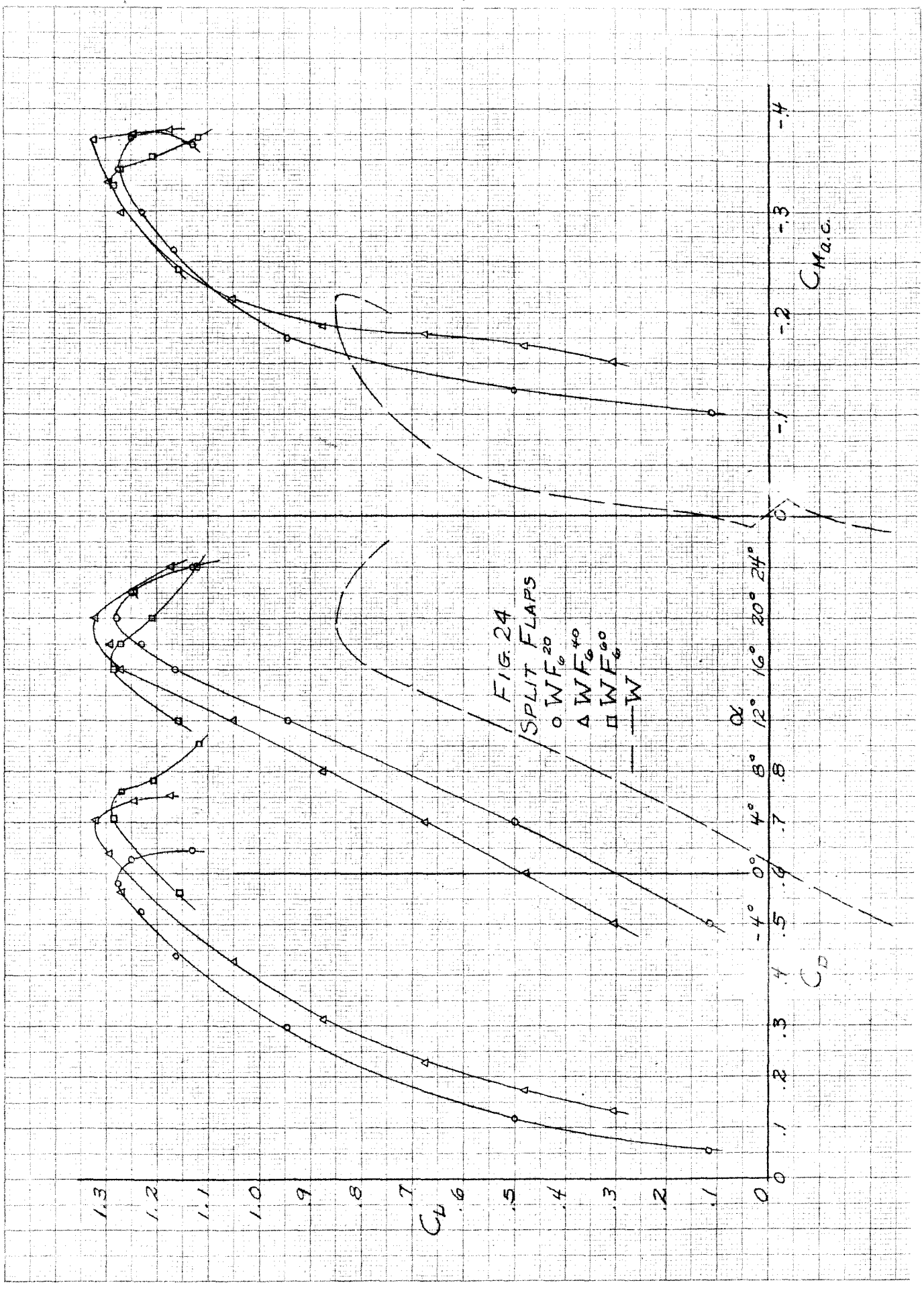
FIG. 24
SPLIT FLAPS
○ WF δ20
△ WF δ40
□ WF δ60
— W
α -4° 0° 4° 8° 12° 16° 20° 24°
CL
CD
Cm a.c.

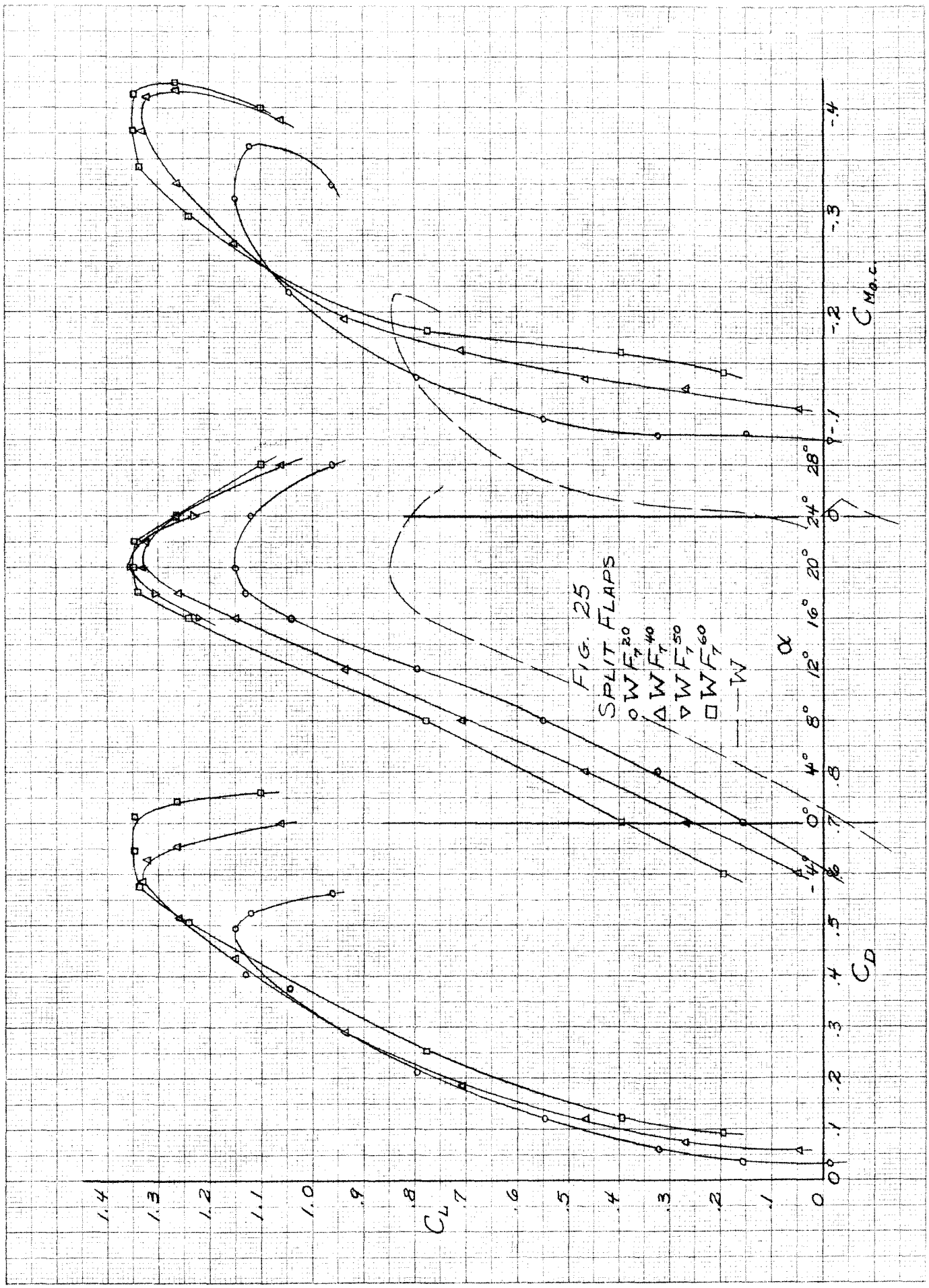
FIG. 25
SPLIT FLAPS
○ WF 20
△ WF 40
▽ WF 50
□ WF 60
—— W
α
C_L
C_D
$C_{M_{c/4}}$

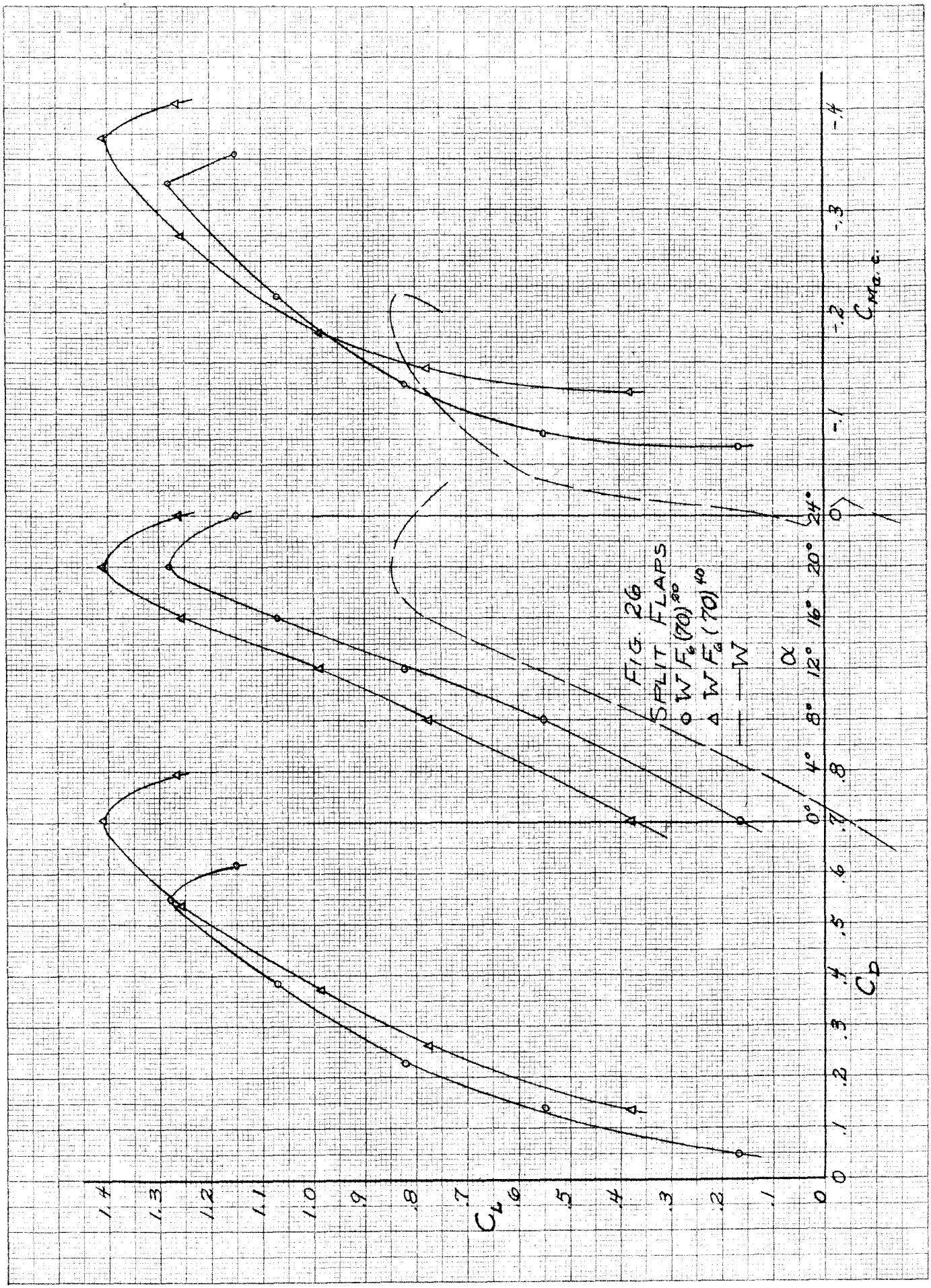
FIG. 26
SPLIT FLAPS
○ W F_e (70) 80
△ W F_a (70) 40
—— W
C_L
C_D
$C_{M_{a.c.}}$
α
0° 4° 8° 12° 16° 20° 24°
0 .1 .2 .3 .4 .5 .6 .7 .8 .9 1.0 1.1 1.2 1.3 1.4
-.1 -.2 -.3 -.4

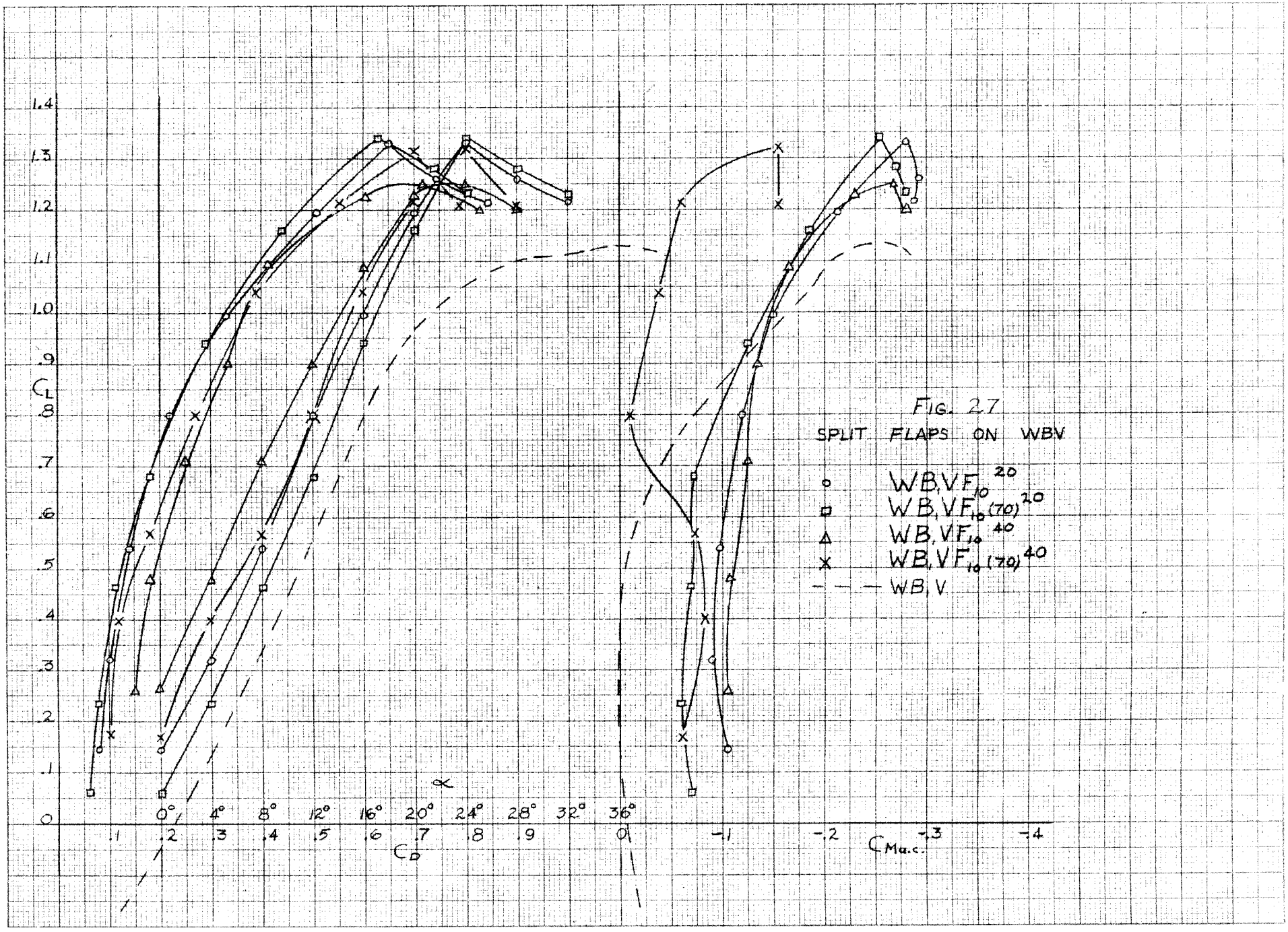

FIG. 27

SPLIT FLAPS ON WBV

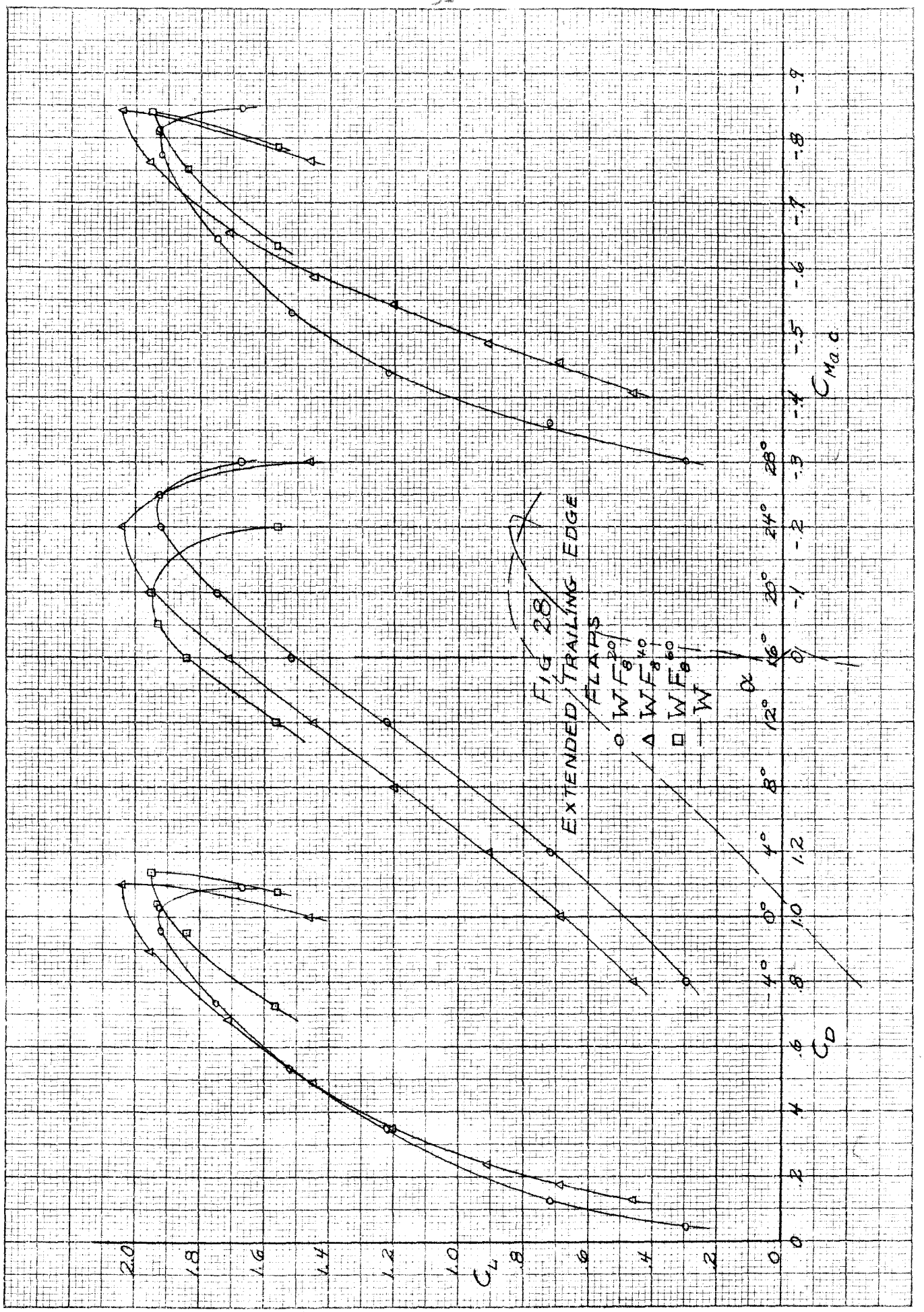
C_L
C_D
$C_{Ma.c}$
α
WF δ20
WF δ40
WF δ60
— W
EXTENDED TRAILING EDGE FLAPS

FIG 28

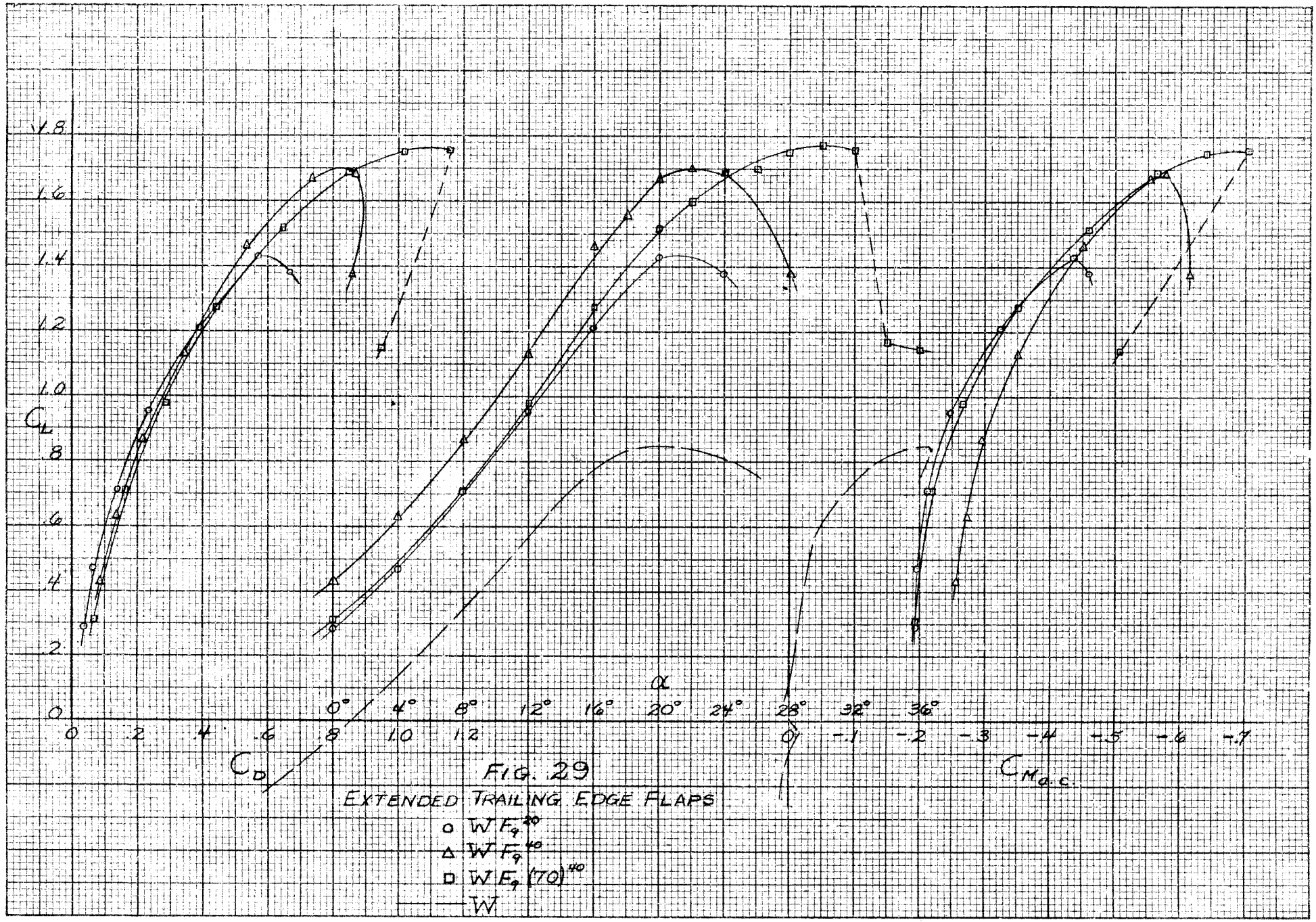

FIG. 29

EXTENDED TRAILING EDGE FLAPS

- ○ WF_9^{20}
- △ WF_9^{40}
- □ $WF_9(70)^{40}$
- —— W

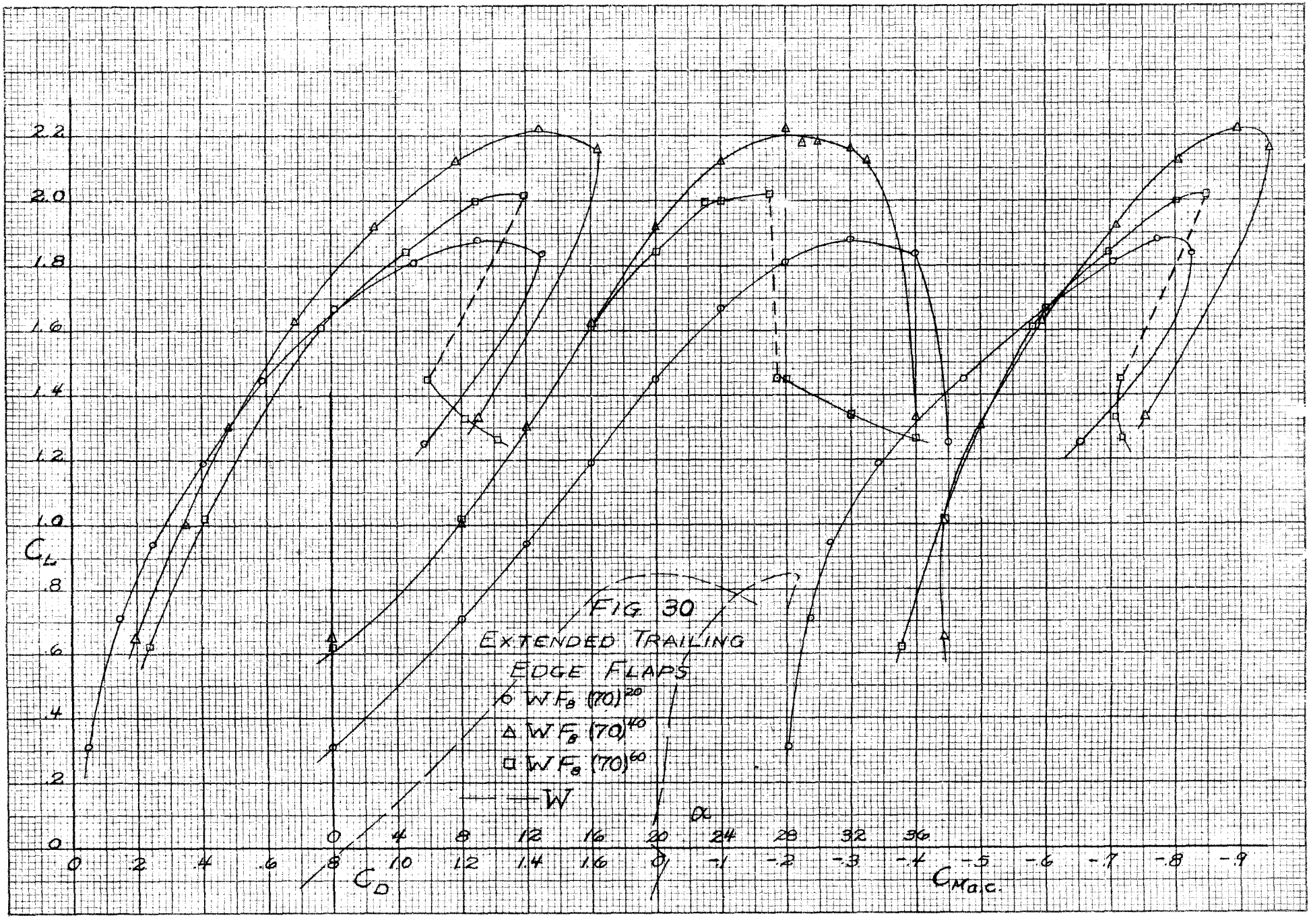
2.2
2.0
1.8
1.6
1.4
1.2
1.0
C_L
.8
.6
.4
.2
0
0 .2 .4 .6 .8 1.0 1.2 1.4 1.6
C_D
0 4 8 12 16 20 24 28 32 36
α
0 -1 -2 -3 -4 -5 -6 -7 -8 -9
$C_{M_{a.c.}}$
FIG 30
EXTENDED TRAILING
EDGE FLAPS
○ $WF_8(70)^{20}$
△ $WF_8(70)^{40}$
□ $WF_8(70)^{60}$
—— W

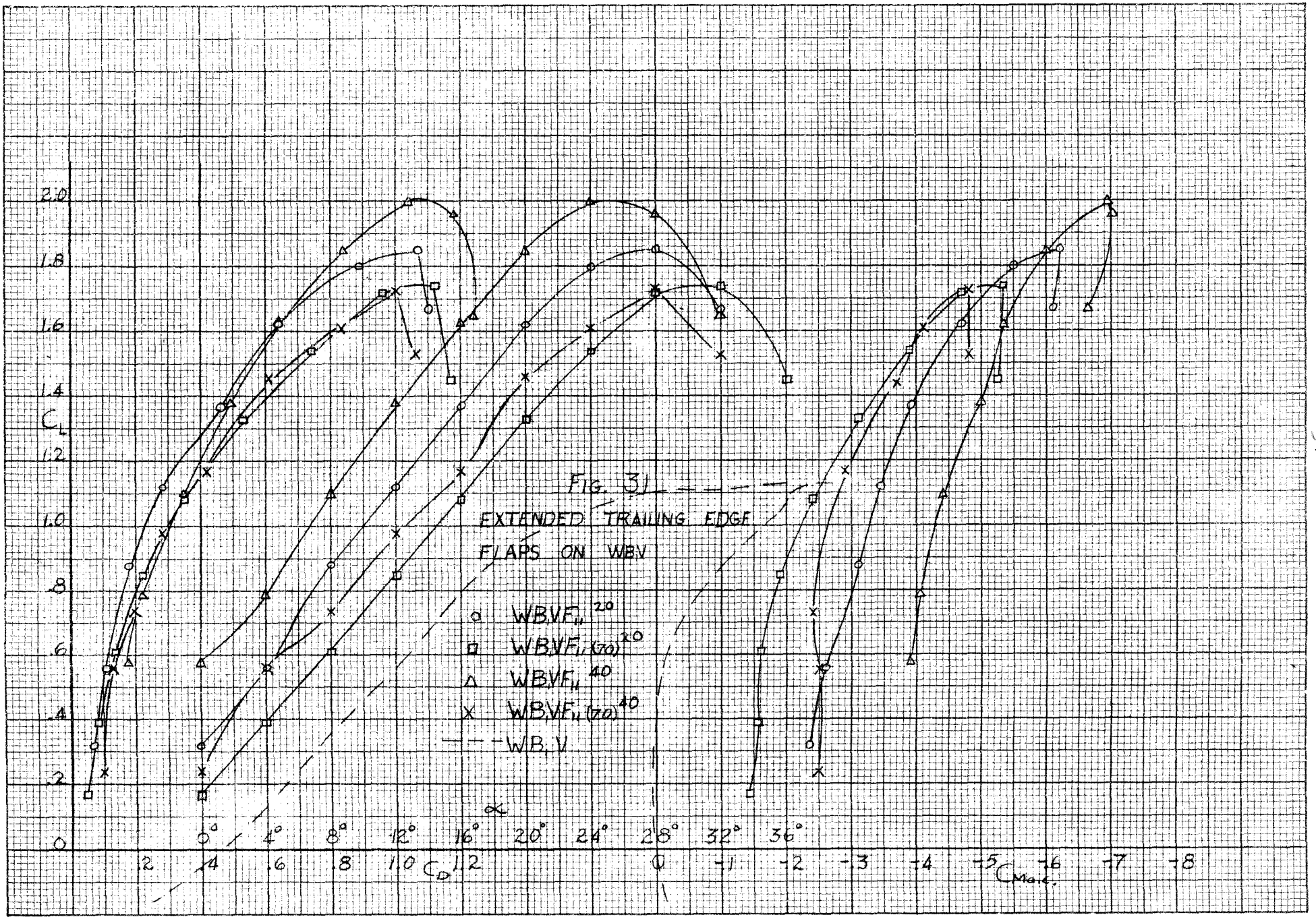
2.0
1.8
1.6
1.4
C_L
1.2
1.0
.8
.6
.4
.2
0
FIG. 31
EXTENDED TRAILING EDGE
FLAPS ON WBV
$WBVF_{II}^{20}$
$WBVF_{I(70)}^{20}$
$WBVF_{II}^{40}$
$WBVF_{II(70)}^{40}$
WB_IV
α
0° 4° 8° 12° 16° 20° 24° 28° 32° 36°
.2 .4 .6 .8 1.0 C_D 1.2
0 -1 -2 -3 -4 -5 -6 -7 -8 $C_{M_{a.c.}}$

FIG. 32 $C_{L_{MAX.}}$ vs. FLAP DEFLECTION

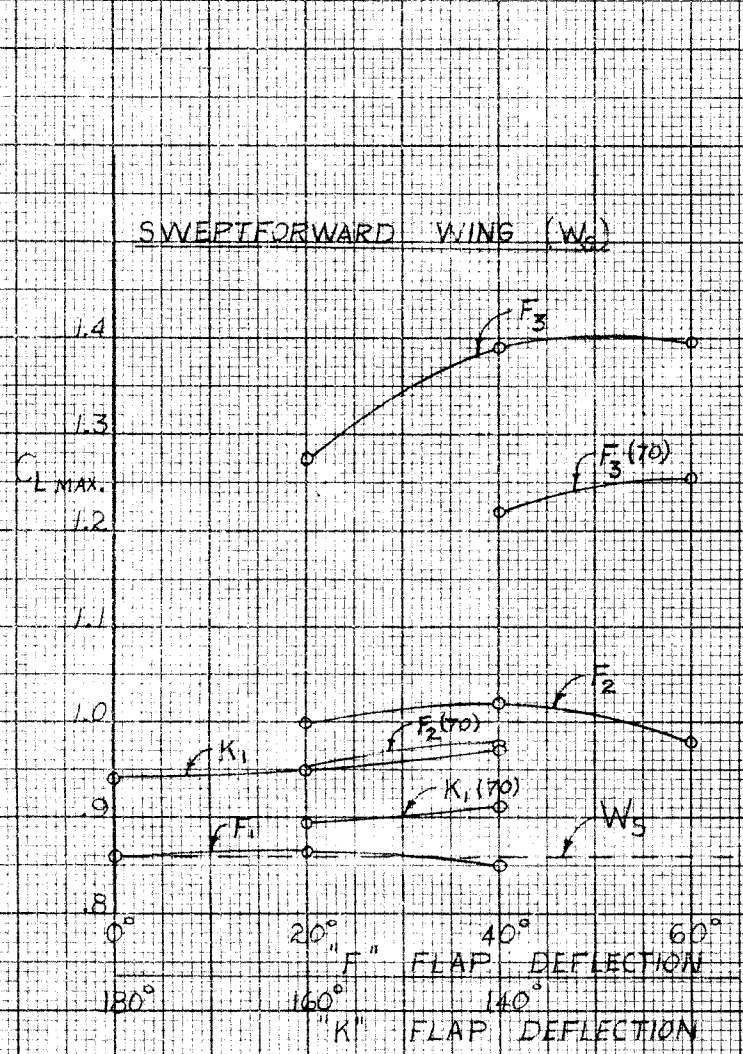

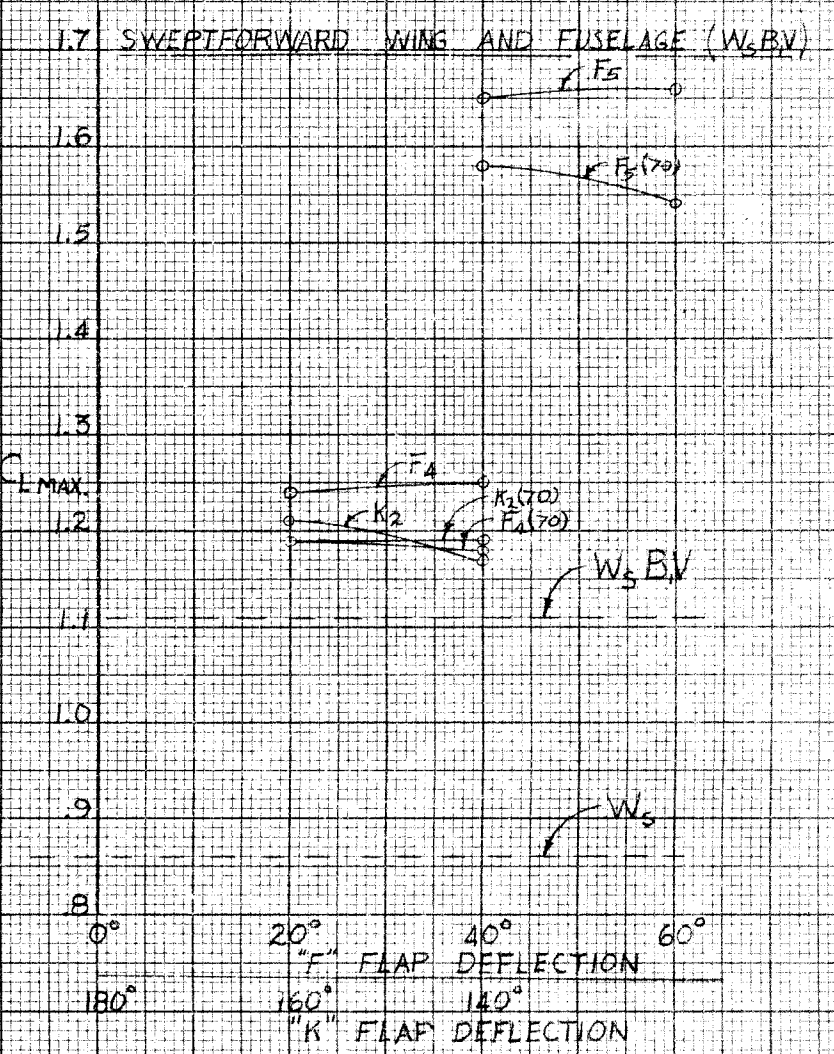

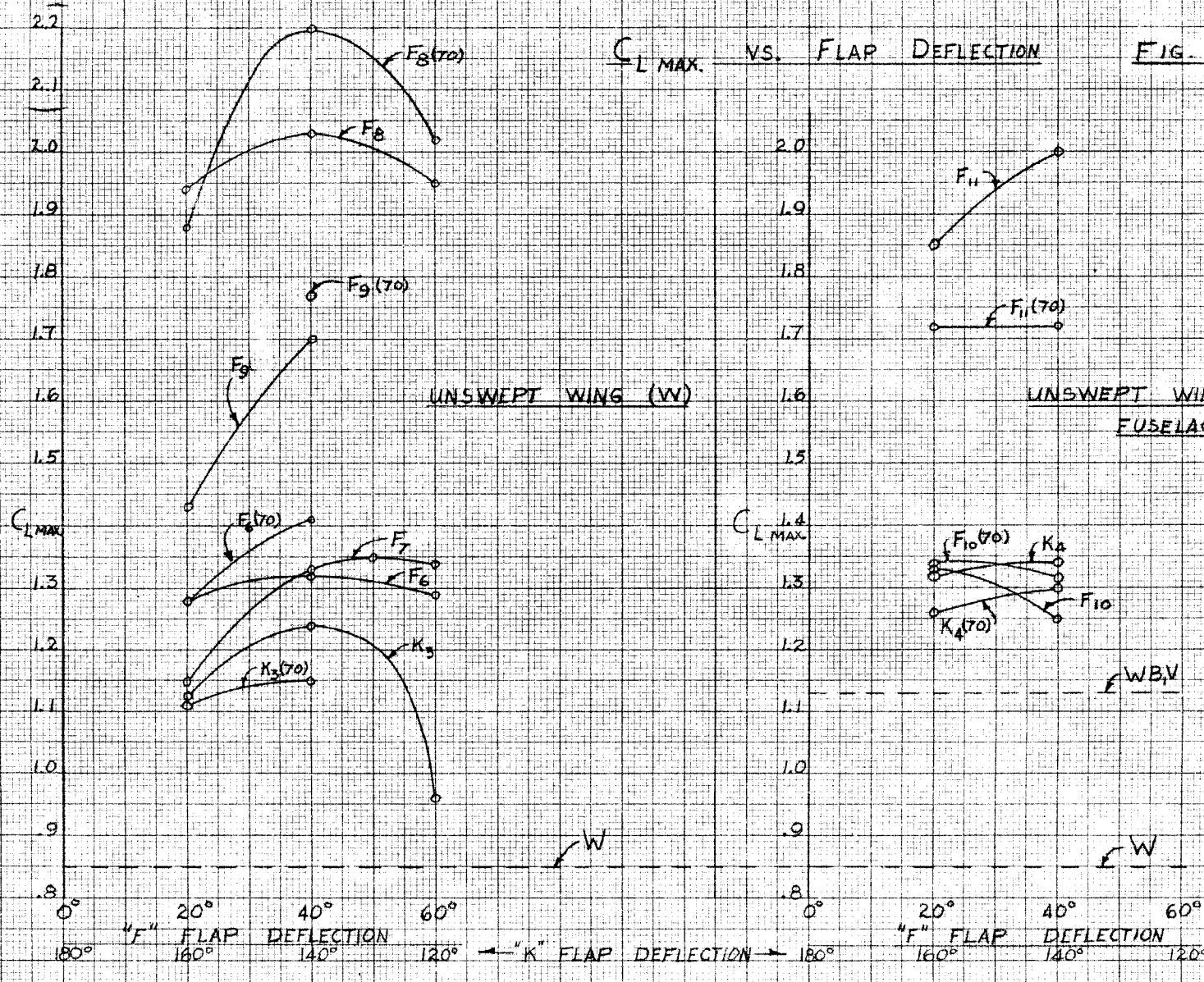
$C_{L\ MAX.}$ VS. FLAP DEFLECTION
FIG. 33
UNSWEPT WING (W)
UNSWEPT WING AND FUSELAGE (WB,V)
$C_{L\ MAX.}$
2.2
2.1
2.0
1.9
1.8
1.7
1.6
1.5
1.4
1.3
1.2
1.1
1.0
.9
.8
$F_8(70)$
F_8
$F_9(70)$
F_9
$F_6(70)$
F_7
F_6
K_3
$K_3(70)$
W
F_{11}
$F_{11}(70)$
$F_{10}(70)$
K_4
F_{10}
$K_4(70)$
WB,V
0°
20°
40°
60°
"F" FLAP DEFLECTION
180°
160°
140°
120°
"K" FLAP DEFLECTION

Fig. 34

W

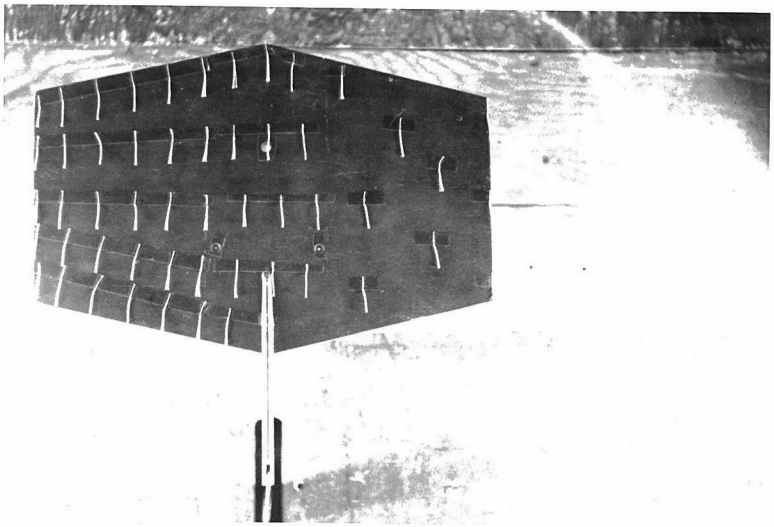

$\alpha = 0°$

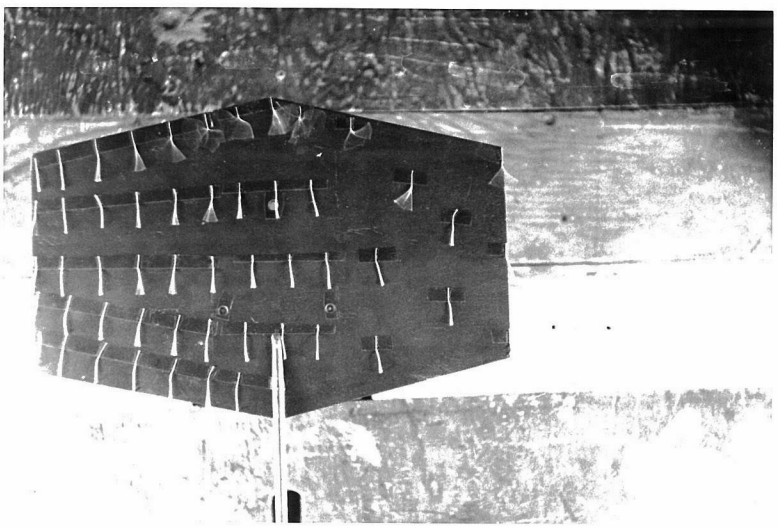

$\alpha = 5°$

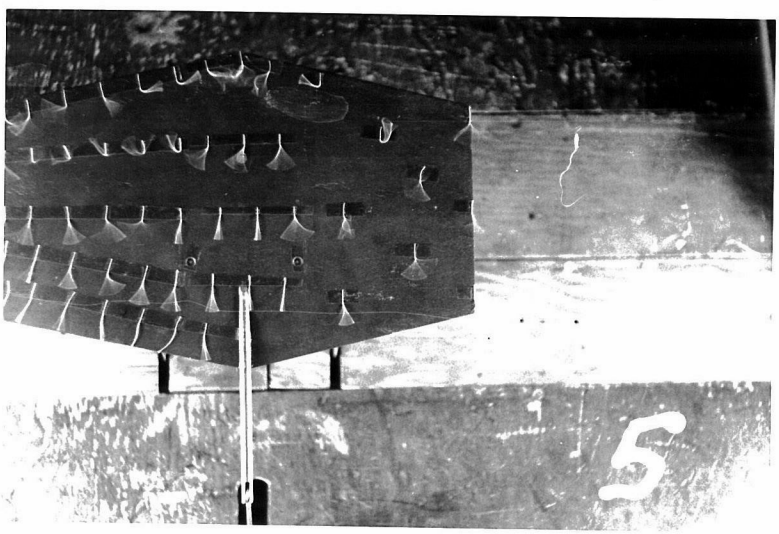

$\alpha = 12°$

Fig. 35

W

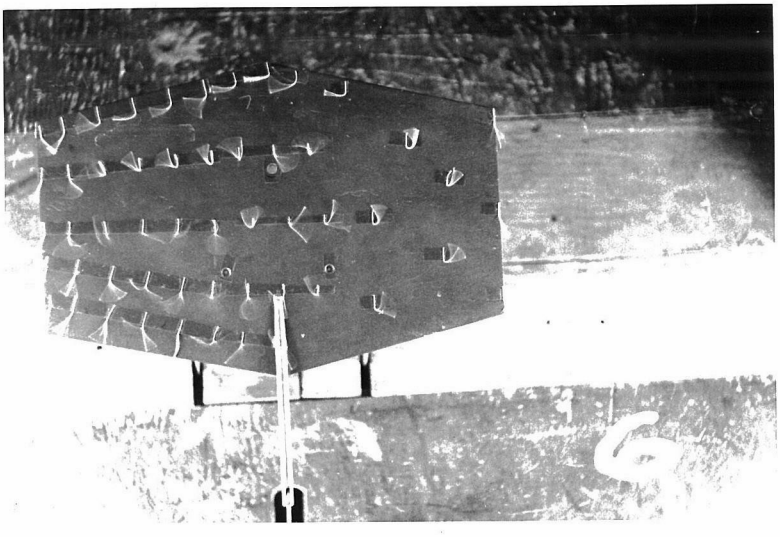

$\alpha = 15°$

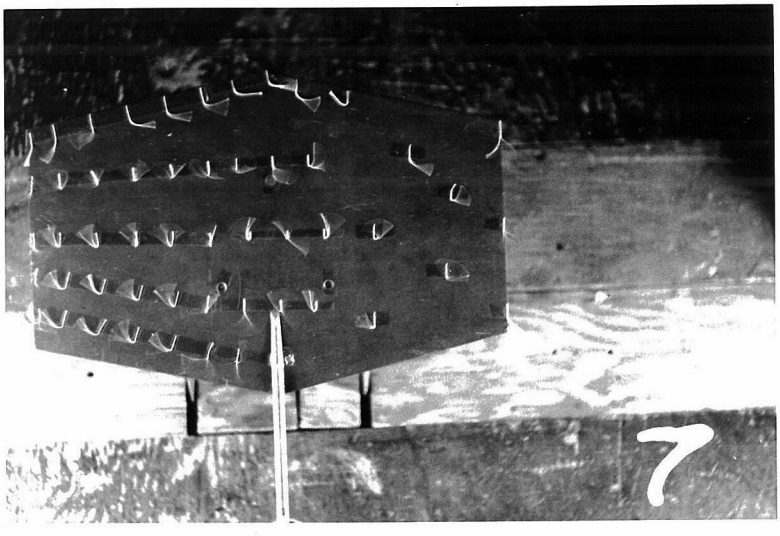

$\alpha = 20°$

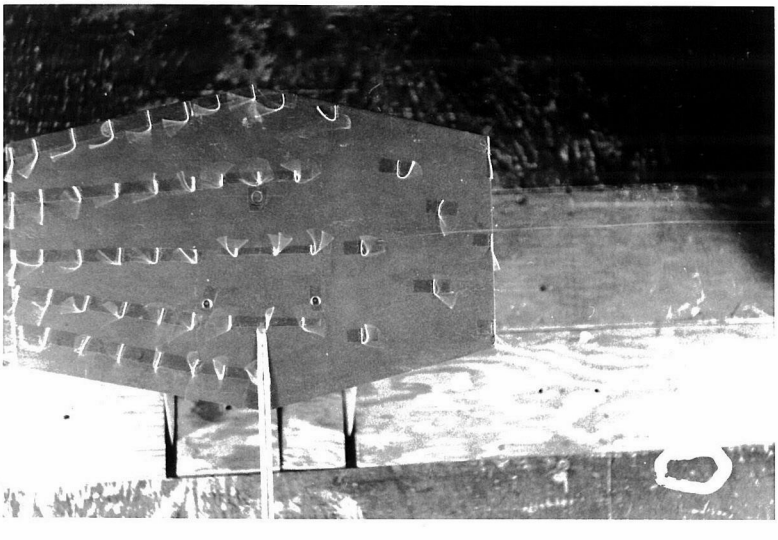

$\alpha = 28°$

Fig. 36

WB_1V

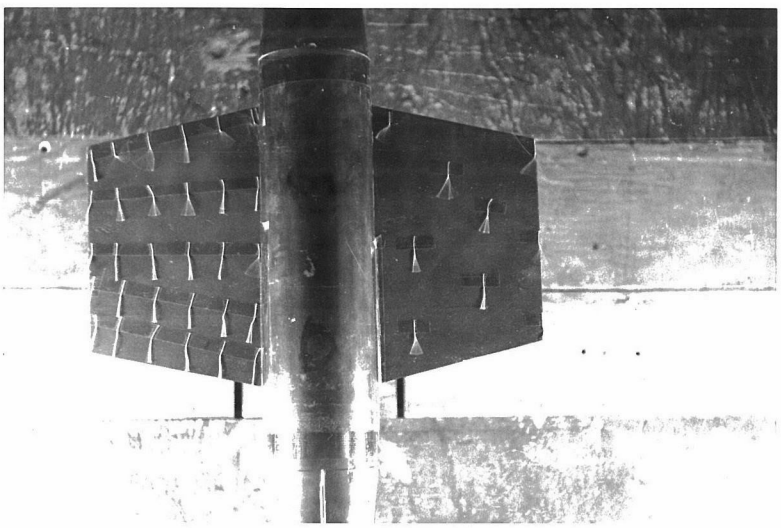

$\alpha = 8°$

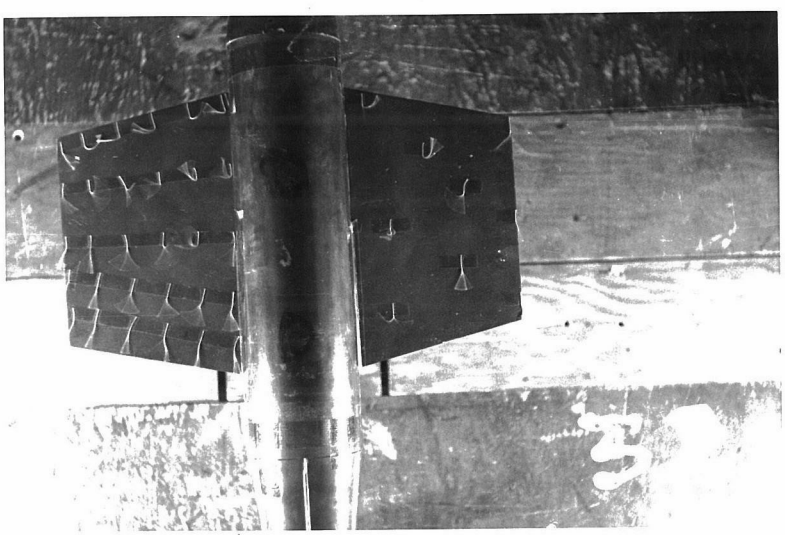

$\alpha = 10°$

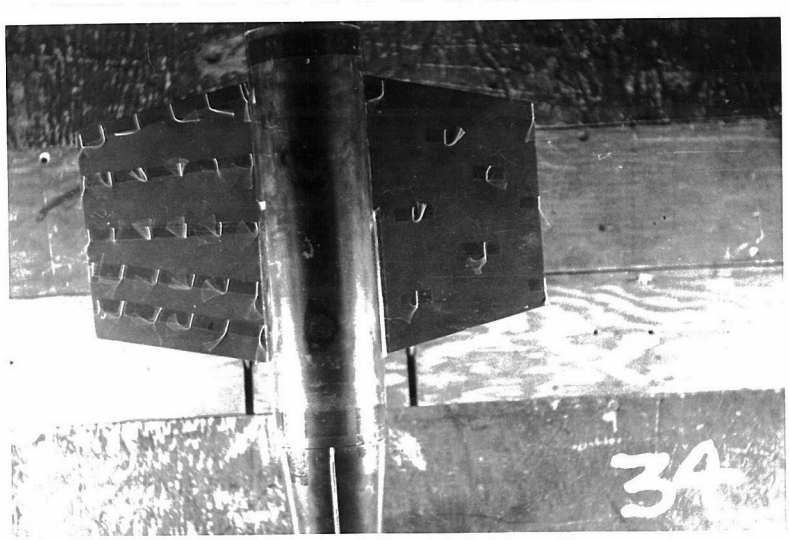

$\alpha = 18°$

Fig. 37

WB_1V

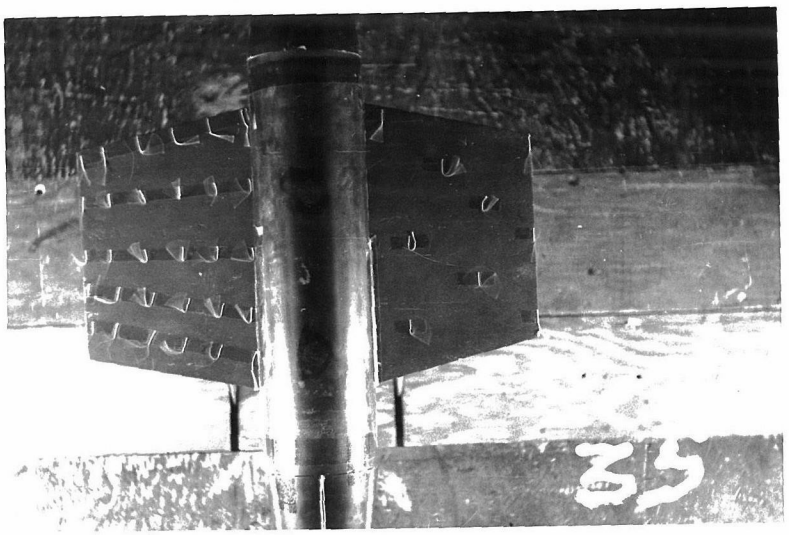

$\alpha = 20°$

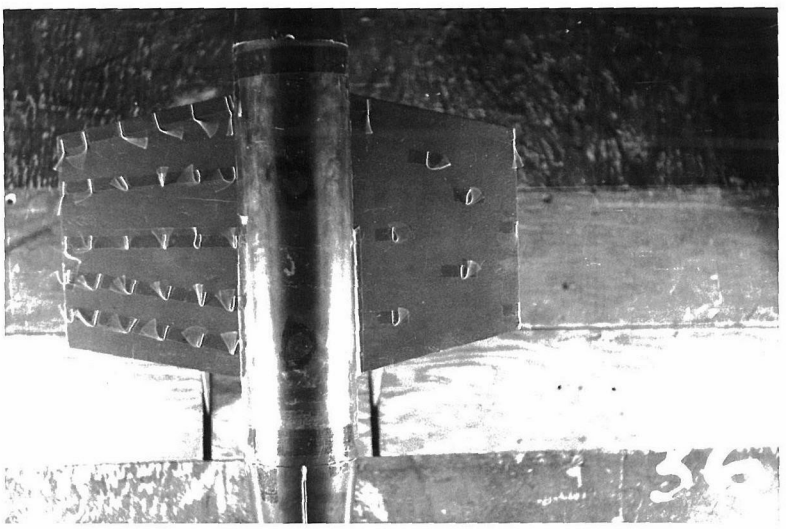

$\alpha = 26°$

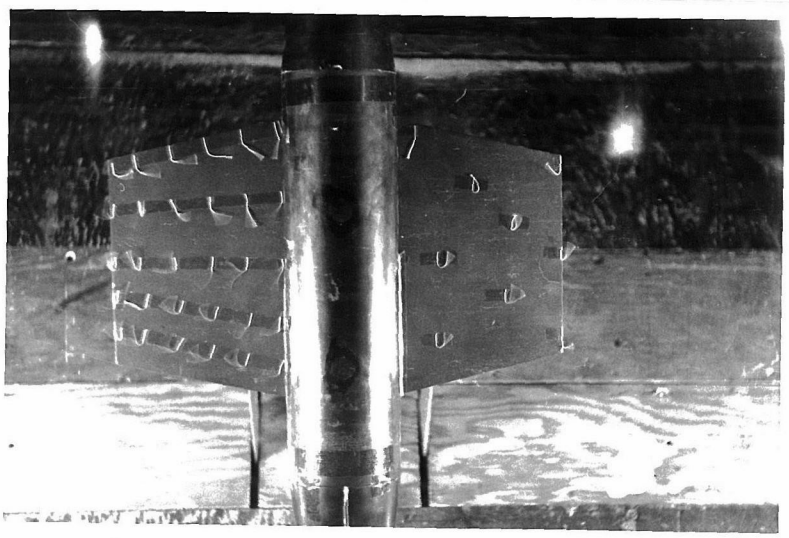

$\alpha = 36°$

Fig. 38

W_s

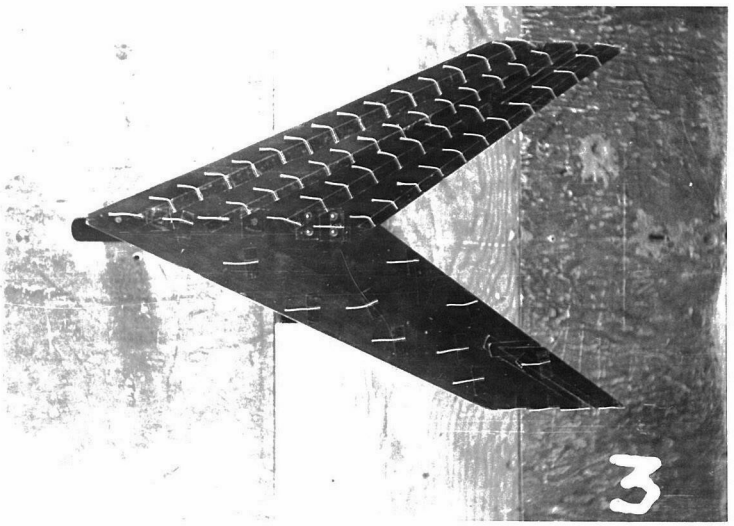

$\alpha = 0°$

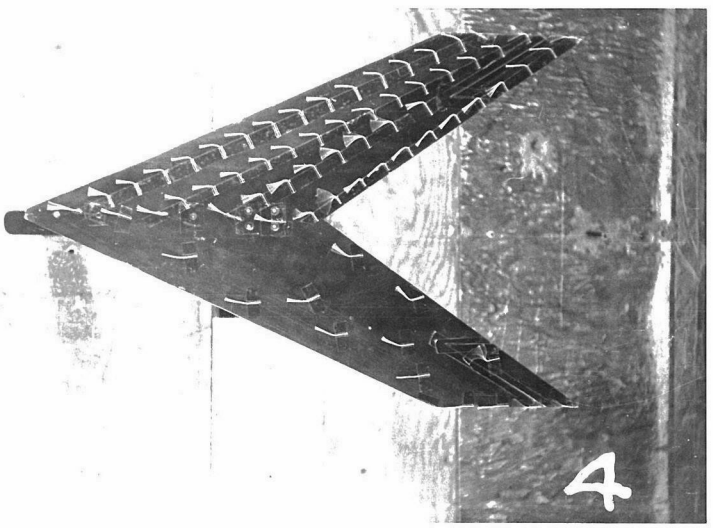

$\alpha = 8°$

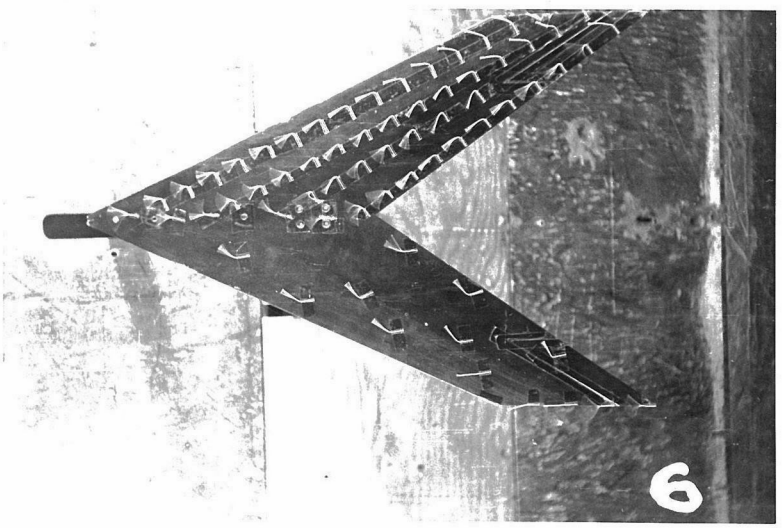

$\alpha = 24°$

Fig. 39

W_s

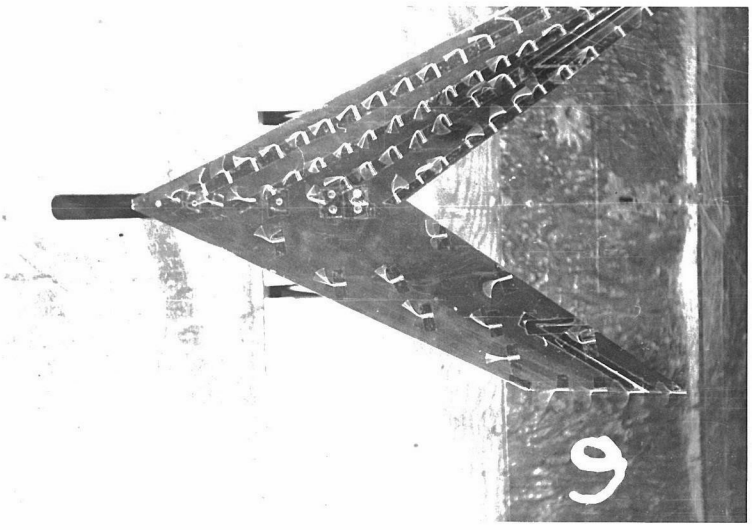

$\alpha = 34^\circ$

Fig. 40

$W_s B_1 V$

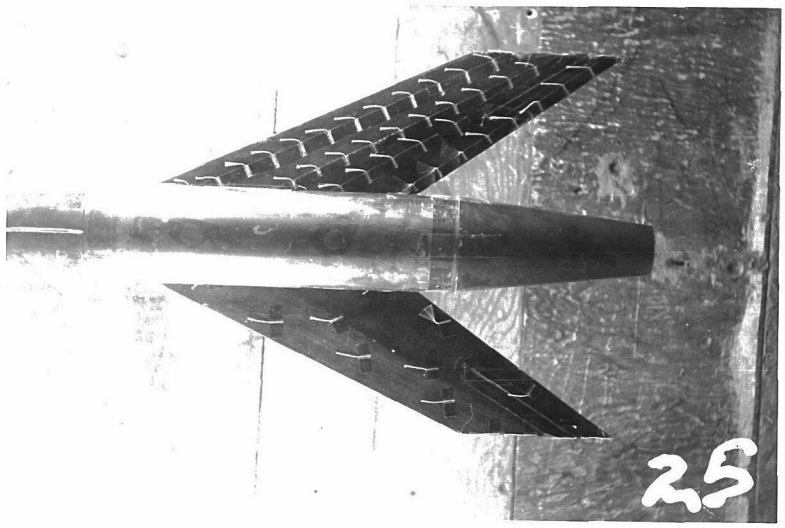

$\alpha = 7°$

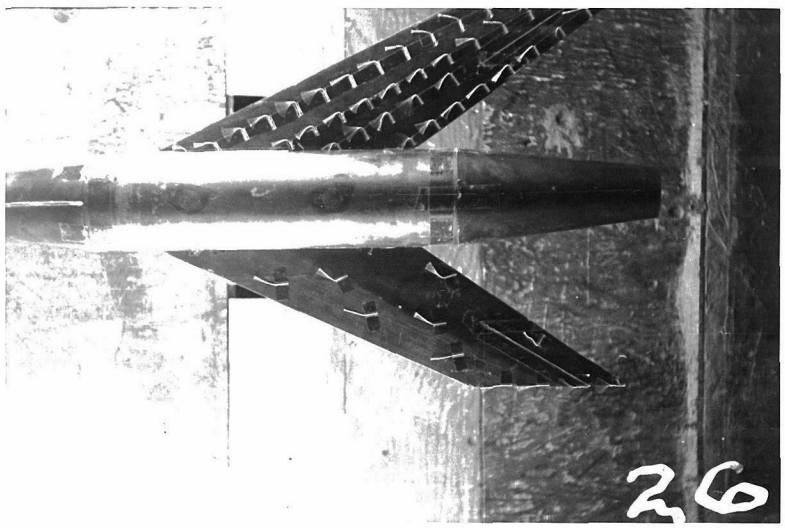

$\alpha = 20°$

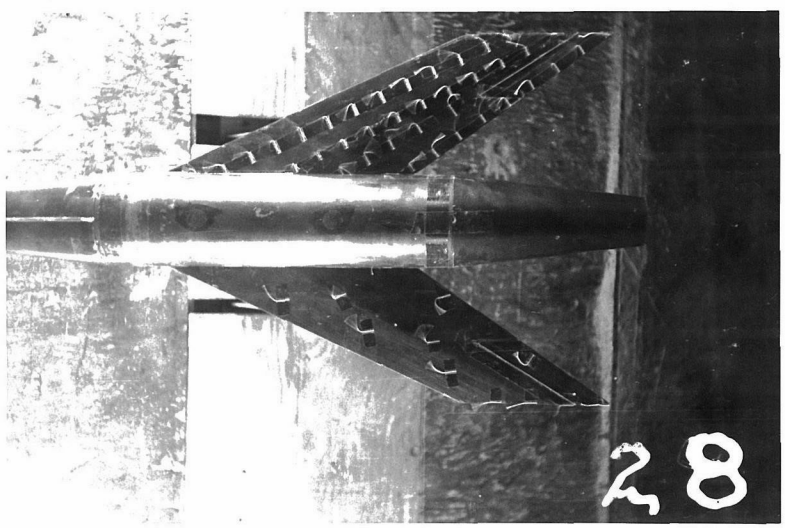

$\alpha = 31°$

Fig. 41

$W_s F_3{}^{40}$

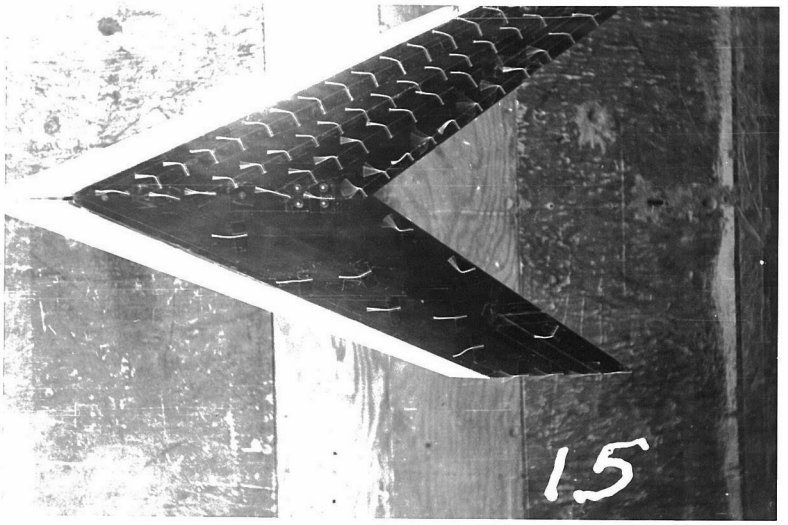

$\alpha = 6°$

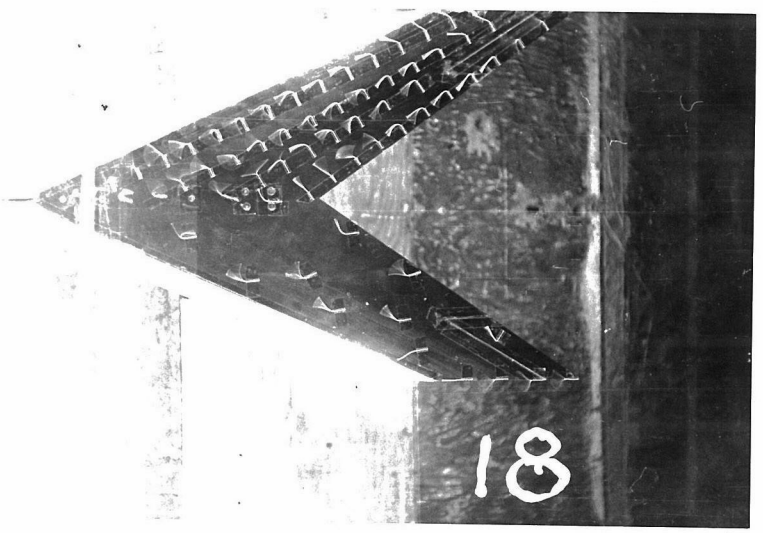

$\alpha = 26°$

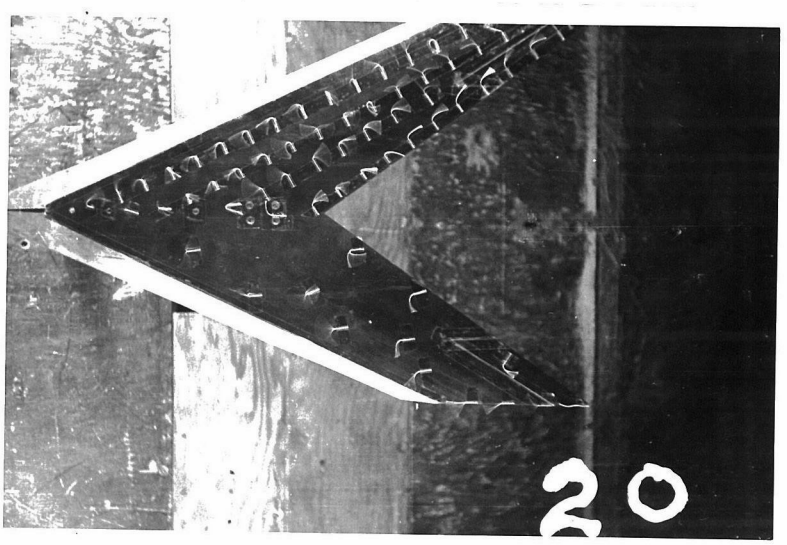

$\alpha = 38°$

Fig. 42
WF_8^{40}

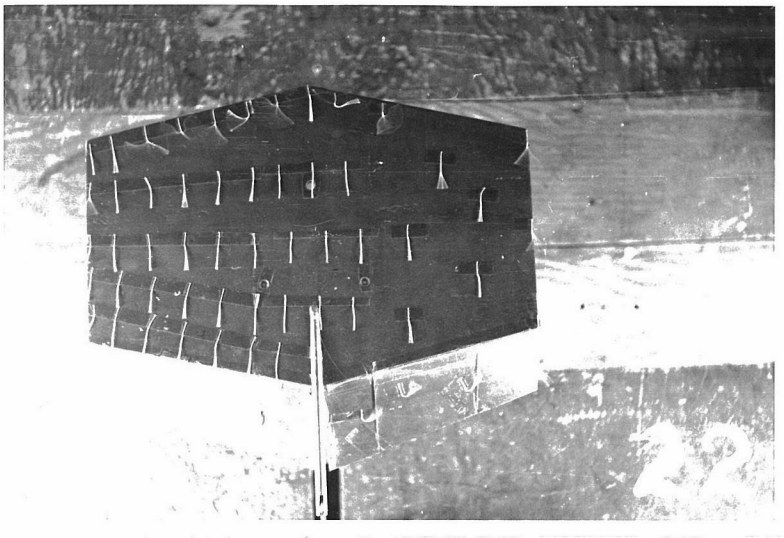

$\alpha = 4°$

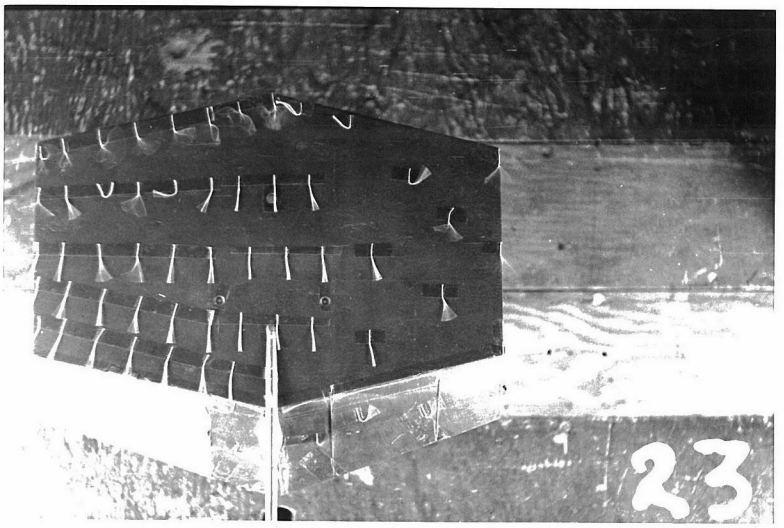

$\alpha = 10°$

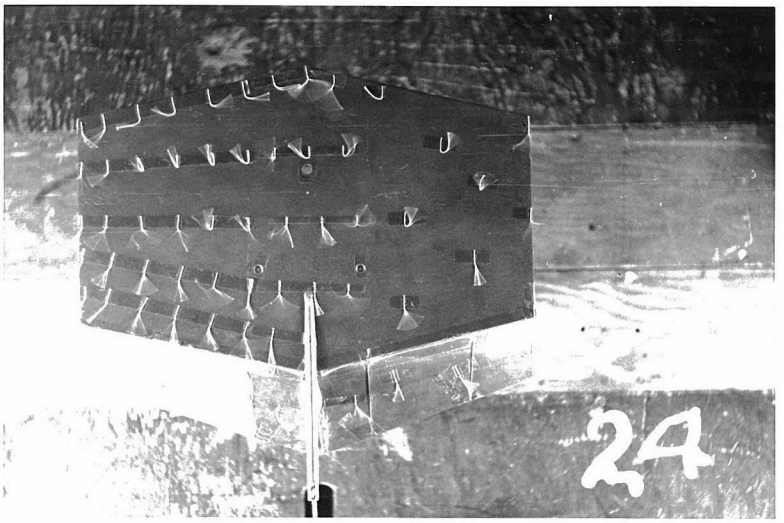

$\alpha = 15°$

Fig. 43

WF_8^{40}

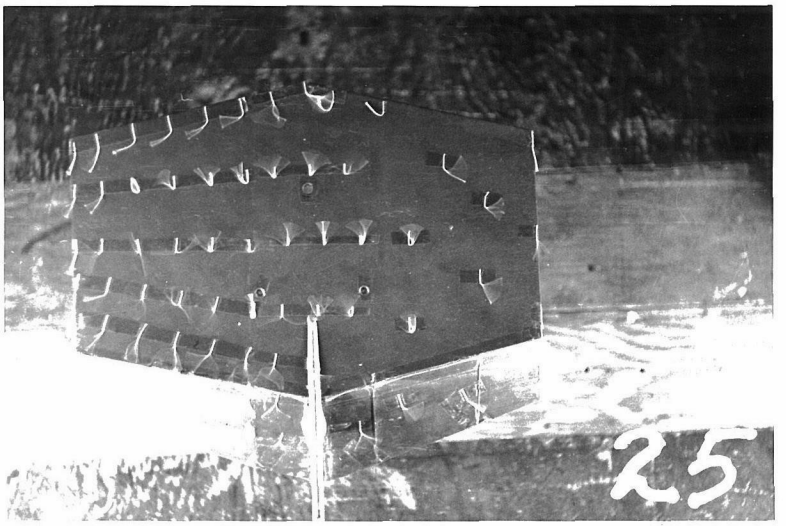

$\alpha = 21°$

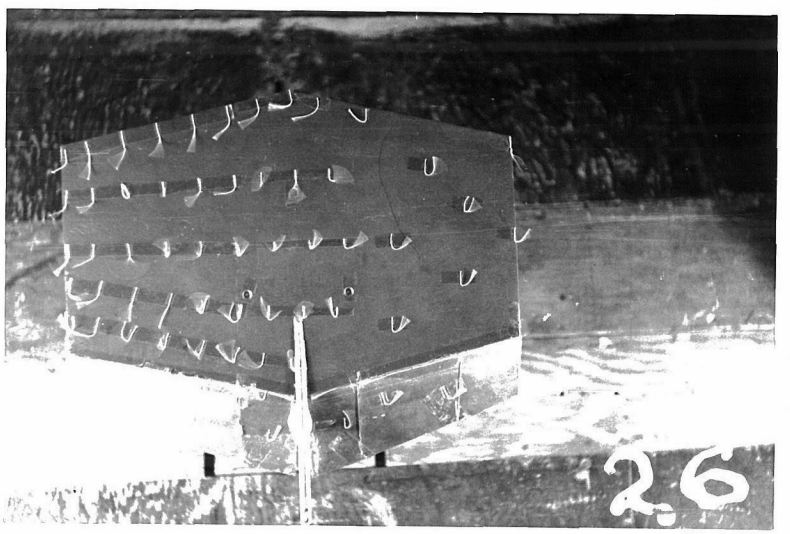

$\alpha = 28°$

Fig. 44

$WF_8(70)^{40}$

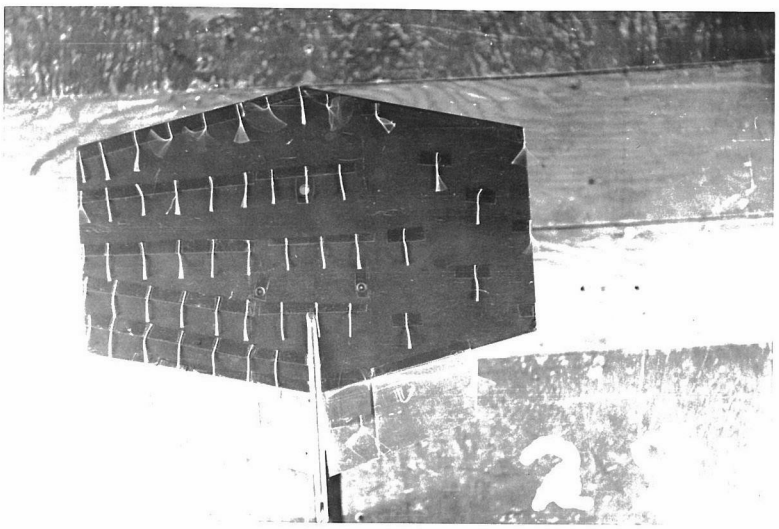

$\alpha = 4^\circ$

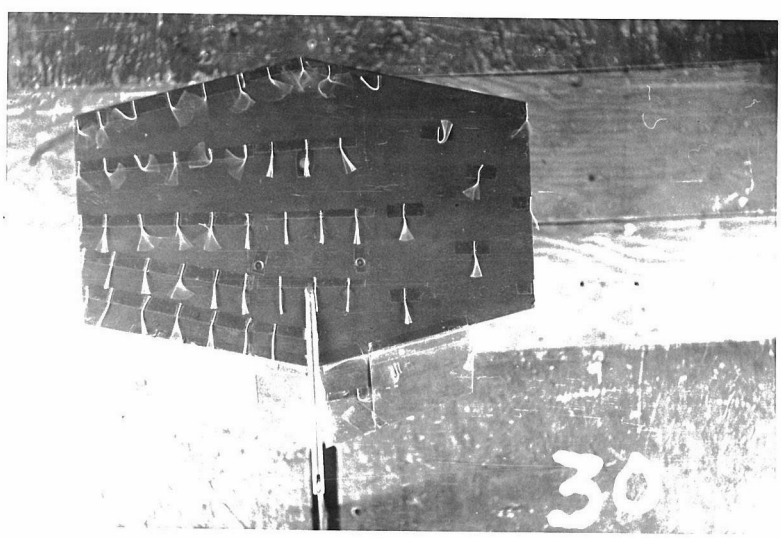

$\alpha = 10^\circ$

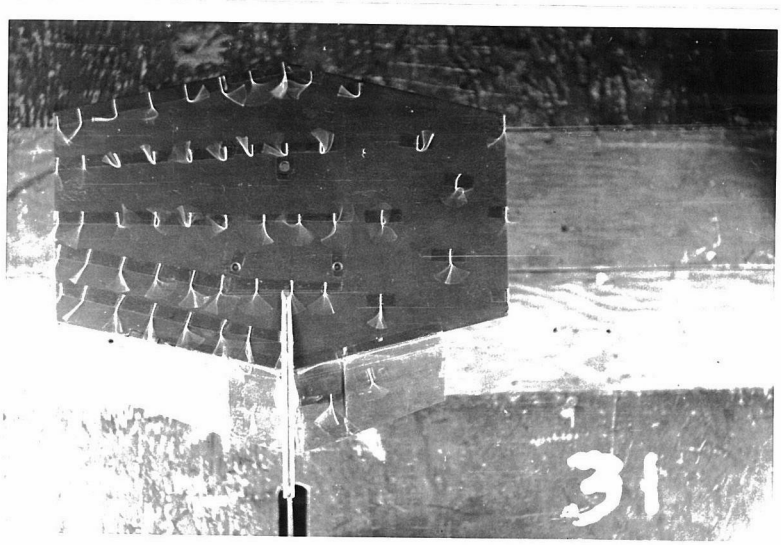

$\alpha = 15^\circ$

Fig. 45

$WF_8(70)^{40}$

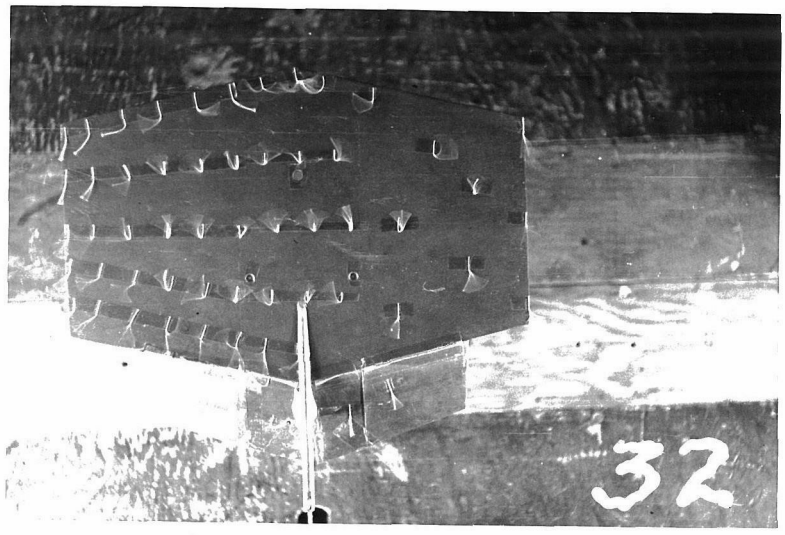

$\alpha = 21^\circ$

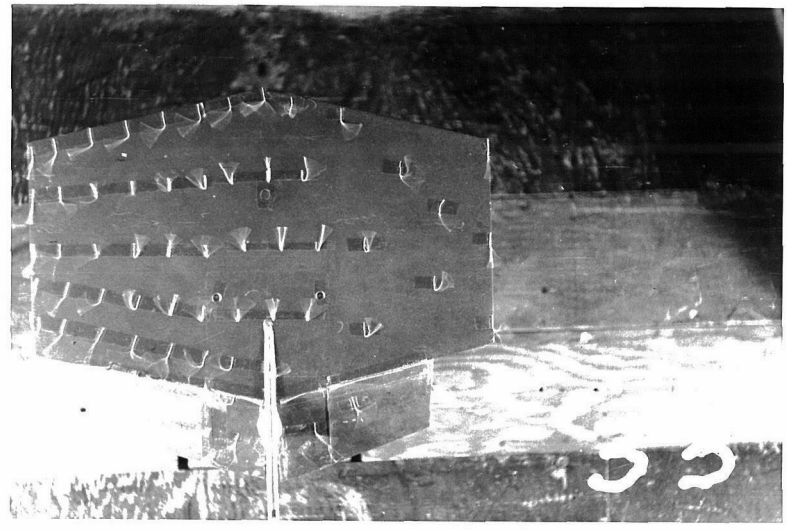

$\alpha = 28^\circ$

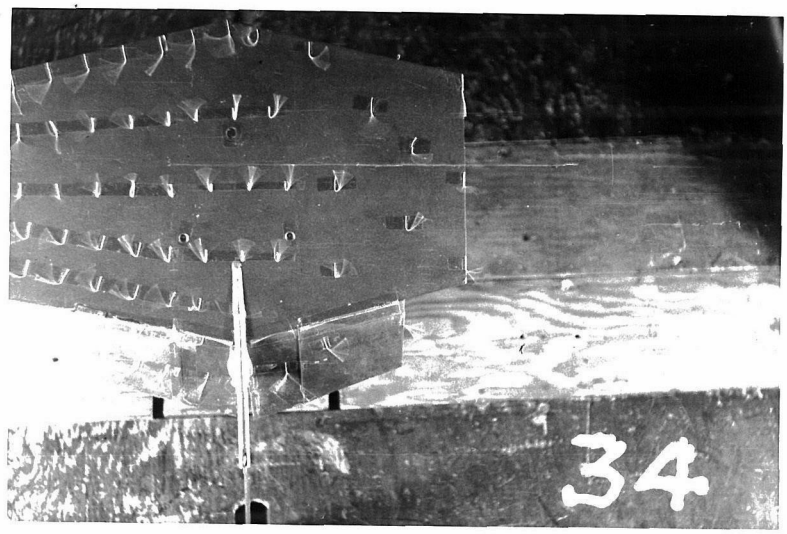

$\alpha = 33^\circ$

Fig. 46

$WF_8(70)^{40}$

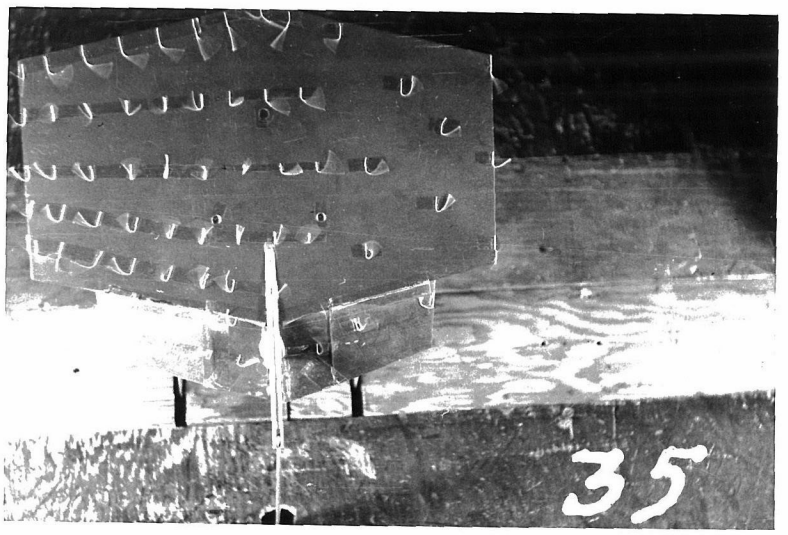

$\alpha = 38^\circ$